Design and performance analysis of electric Tuk-Tuk charging stations powered with renewable energies in South Africa

By

Lindiwe Bokopane

Thesis is submitted in fulfilment of the requirements for the degree:

M. Tech: Electrical Engineering

In the Department of Electrical, Electronic and Computer Engineering

Faculty of Engineering and Information Technology

Central University of Technology

Supervisor**: Dr K. Kusakana**

Co-supervisor: **Prof. H.J. Vermaak**

Bloemfontein 2015

Declaration

I Lindiwe Bokopane (Identity number 860816 0425 080, student number 205030386) do hereby declare that the dissertation submitted for the degree of Master Technologiae: Electrical Engineering is my own independent work and it complies with the Code of Academic integrity, as well as other relevant policies procedures, rules and regulation of the Central University of Technology; and has not been previously submitted to any other institution of higher education.

L. Bokopane

Dedication

To Jesus Christ my lord and saviour for every blessing bestowed upon me.

Acknowledgements

The Author would like to thank the following individuals and institution, without whom the completion of this dissertation would have not been a possibility:

First and foremost I would like to thank God almighty for blessing me with all the opportunities in my life, Then too my late mother, Masentle Lorna Rasiile, who was a pillar of strength and a driving force behind my studies and every one in my family who supported and encouraged me to finish what I had started. Sincerest thanks also go to Dr K Kusakana and Prof H.J Vermaak for their mentoring and guidance, and to the CUT for granting me the opportunity to undertake this project.

Abstract

The success of renewable powered electric vehicle charging stations in isolated areas depends highly on the availability and sustainability of renewable resources all year round at selected locations. A hybrid renewable energy system (HRES) is a viable option for isolated standalone off-grid areas. The HRES should be incorporated with an energy storage system (ESS), which will be utilised as a storage unit when the generated energy at the station exceeds the load requirements. The ESS will also serve as a backup energy supply system, when the HRES is unable to meet the load requirements. Research has indicated that the most reliable, efficient and flexible energy storage system for HRES is rechargeable batteries. However, frequent discharge cycling utilisation of battery banks imposes a penalty on the battery life span. The rate of discharging and charging the battery bank will either increase/decrease the maintenance and replacement cost.

This study will have two major purposes: (1) will be to investigate the possible charging strategies that could be implemented to find the best possible configuration of an electric Tuk-Tuk charging station in the rural areas, and isolated islands of South Africa. The charging station will be designed, modelled and simulated to evaluate its performance. The techno-economic analysis of different feasible supply configurations of the charging station using renewable energies will be simulated using HOMER energy software, and the results will be compared in order to select the most viable charging strategies in terms of the cost of energy (COE) produced. (2) Will be to investigate the possibilities of controlling and optimising the daily operation of a standalone hybrid renewable energy system by maximising the usage of the renewable resources whilst minimising the utilisation of the battery bank for supplying the required energy at an electric Tuk-Tuk charging station without any load rejection. The effectiveness and efficiency of the proposed control strategy will be performed and simulated using *fmincon* in a MATLAB environment. The results for different scenarios will be presented and analysed for different potential sites in the rural parts of South Africa where the charging stations could be sited.

Keywords:

Battery banks, cost minimization, electric vehicle charging station, energy management system, hybrid renewable energy, optimal operation control, and optimisation algorithm.

Table of Contents

List of figures

List of tables

Acronyms and abbreviation

AC	Alternating current
BCS	Battery charging station
BES	Battery energy system
BESS	Battery energy storage system
BEV	Battery electric vehicle
BMS	Battery management system
BSS	Battery swapping station
CHADEMO	Charge De Move
COE	Cost of energy
CO_2	Carbon dioxide
DC	Direct current
DG	Diesel generator
DRC	Democratic republic of Congo
EMS	Energy management system
EREV	Extended-range electric vehicle
ESS	Energy storage system
ETT	Electric Tuk-Tuk
EV	Electric vehicle
EVSC	Electric vehicle charging station
EVSE	Electric vehicle supply equipment
HEV	Hybrid electric vehicle
HRES	Hybrid renewable energy system
HOMER	Hybrid optimisation modelling software

IEC	International electro-technical commission
ICE	Internal combustion engine
IGBT	Insulated gate bipolar transistor
MATLAB	Matrix laboratory
NEV	Neighbourhood electric vehicle
NiCad	Nickel cadmium
NiMH	Nickel metal hydride
PEV	Plug-in electric vehicle
PHEV	Plug-in hybrid electric vehicle
PMS	Power management system
PV	Photovoltaic
RETScreen	Clean energy project analysis software
SAE	Society of automotive engineers
SOC	State of charge
THD	Total harmonic distortion

Chapter I: Introduction

1.1 Introduction

South Africa faces significant public transport challenges, with the vast majority of rural and township occupants relying on public transport, making this form of transport a critical tool for getting the workforce to and from work in order to avoid disruption to economic activities [1]. In recent years the population, as well as the country's economy, has grown, so the demand for passenger transport, electricity, water, sanitation and private vehicles has increased [2]. The transportation sector is a large consumer of energy in South Africa and it is vital for economic development, hence making the provision of affordable, safe and reliable transportation of goods and people critical to the development of the country [2].

A number of transportation modes have been introduced in our country over the years to combat the challenge associated with transport, comprising buses, taxis, trains, trucks as well as Tuk-Tuks. Of all these modes of transportation, the Tuk-Tuk is better suited for rural areas as it can be driven in mountainous and rocky areas with the greatest of ease.

Tuk-Tuks are portable and reliable three-wheeled vehicles which have been used for over 60 years in Asian, European, Central American, South American and in some African countries, and where introduced to our roads due to their efficiency , stylistic simplicity, low fuel consumption, they have demonstrated flexibility; light-weight, excellent manoeuvrability; lower travel costs and inexpensive operational costs [3-4].

However they pose a huge pollution threat, due to their inefficient engine with almost no pollution control. They emit gaseous substances, like carbon dioxide, carbon monoxide, particulate matter, sulphur dioxide as well as nitrogen oxides from the internal combustion engines through their exhaust systems, but that could be remedied as research has shown that Tuk-Tuks are relatively ideal for electrification; and that could be achieved by replacing their internal combustion engines with an all-electric counterpart [4].

According to the environmental statistics, South Africa is among the top 20 countries in the world with high emission levels of carbon dioxide and it is the largest emitter in Africa, largely because of the economy's dependence on fossil fuels. Our country's economy depends on fossil fuels for energy generation and consumption. It is therefore a significant emitter due to relatively high values being derived from emission intensity, as South Africa emits 460.124 million tonnes, followed by Algeria with 107.28 million tonnes per capita out of the 1157.71 million tonnes emitted by the whole African continent [5-7].

The existence as well as the availability of electricity in most rural areas in South Africa, has proved to be a challenge, hence the provision of a standalone hybrid renewable energy (such as photovoltaic, wind or a PV + wind) charging station for recharging electric Tuk-Tuks should be considered as essential for ensuring an uninterrupted power supply to the load. The proposed system should have a battery energy storage system (BESS) in place which will be used to store excess energy during off-peak hours and be utilised as a backup when there is a deficit in the renewable energy resource supply at the charging station. However, the rate of charging/discharging of a battery bank as well as its depth of discharge will influence its life span. Frequent discharge will contribute to a reduced life cycle; conversely minimal usage will prolong its life cycle.

This research investigates the possibilities of using electric Tuk-Tuk battery charging stations powered by purely sustainable and renewable energies such as PV and wind integrated with the

BESS/battery banks in the rural areas, and isolated islands of South Africa. The techno-economic analysis of different feasible supply configurations of a charging station using renewable energies will be simulated using HOMER energy software and the results of the cost of energy (COE) produced will be compared using different systems configurations such as a PV system, wind system and hybrid energy system (PV + wind) while responding to the battery charging energy requirements of the Tuk-Tuk. Different strategies for operating the charging station will be simulated; the results will be analysed and discussed in order to select the best system configuration.

The second part of this research investigates the possibilities of controlling and optimising the daily operation of a standalone HRES, by maximising the usage of the renewable resources whilst minimising the utilisation of the battery bank for supplying the required energy at the electric Tuk-Tuk charging station without any deficit in the load demand. The control and optimal energy management of an isolated electric Tuk-Tuk charging station will be performed and simulated using fmincon in a MATLAB environment. The results will then be presented, compared and analysed in order to select the best possible system configuration which offers minimal battery usage and maximum usage of the HRES.

1.2 Problem statement

- There are isolated rural areas in South Africa where the transport of goods and persons is poorly developed and the traditional way of transport using a vehicle with combustion engine is not economic due to the ongoing reliance on fossil fuel, which also induces a problem of pollution due to gas emission.

- The technology of an electric vehicle charging station and its developed standards are not readily applicable in rural areas with poor or non-existent grid connection.
- Frequent charging and discharge of the battery banks contribute to a reduced life cycle.

1.3 Objective of the study

The first objective of this research study is to investigate the possibilities of using a standalone off-grid charging station for an electric Tuk-Tuk powered by a hybrid combination of renewable energy sources such as PV and wind and BESS in the rural areas, and isolated islands of South Africa.

This part of the study will strive:

- To design, model and simulate the proposed system,
- To present an economic and environmental analysis of the proposed system,
- To present different operational strategies in order to select the best approach corresponding to the system configuration, load demand as well as renewable energy available.

The second objective of this study is to develop an optimisation model which will be employed to ensure that the energy stored in the battery banks is only utilised when the renewable energies are not producing enough energy to sustain the load at the charging station.

This part of the study will entail:

- Formulating the optimisation problem for the proposed system of minimising the use of BESS and maximising the use of HRES,
- Setting out the objective functions as well as the constraints of the proposed system,

- Formulating a power flow system and power balance,
- Identifying the control variables as well as the battery state of charge limits.

1.4 Limitations of the study

- This study will focus on the charging station aspect, HRES daily operation, the BESS and not on the vehicle.
- The study will also focus on the simulated results of the charging station as well as the simulated optimisation model.

1.5 Expected outcomes

- The main expected outcome of this research is the development of a cost-effective system configuration in terms of COE produced for the electric Tuk-Tuk charging station powered by renewable energies in isolated areas, and to minimise the use of BESS whilst maximising the use of a HRES without any load rejection at the charging station.
- The research results will be documented in a master's thesis as well as in publications.

1.6 Methodology

To achieve the above-mentioned objectives, the methodology is as follows:

- **Literature review:** An in-depth review is done on Electric vehicles technologies, electric vehicle charging station infrastructure, charging times, connector standards, charging station operational strategies, charging station operation principles as well as power generation using renewable energies.

- **Resource Assessment:** A proper investigation of the potential in wind and solar resources will be done at the three selected sites with different resource potential (Upington, Mthatha and Marion Island) in the rural areas, and isolated islands of South Africa where the system can be implemented, to show case which system configuration would be the most viable option (with regards to COE produced) for each location.
- **Vehicle and load analysis:** A thorough investigation of how much energy could be produced using renewable energies (PV and wind), with the South African and its surrounding island weather conditions in mind, to fully charge the batteries of a single electric Tuk-Tuk and to have a daily estimation of how much energy should be produced to cater for the charging requirements at the electric Tuk-Tuk charging station.
- **System configuration and sizing of the main components:** A suitable system layout of all the main components that will be utilised in this research study will be sized.
- **Electric Tuk-Tuk charging station system modelling:** The system will be designed, modelled and simulated using HOMER energy software.
- **Energy management system:** The system will be modelled, simulated and designed using fmincon/MATLAB software.
- **Techno-economic and environmental analysis:** A comparison of different supply options and operation strategies will be made to find the most cost-effective and environmentally friendly option.
- **Optimal energy management strategies:** A mathematical model for controlling and optimising the daily operation of a standalone electric Tuk-Tuk charging station powered

by hybrid renewable energies (PV, wind or both) incorporated with BESS will be developed.

1.7 Hypothesis

- The proposed hybrid electric Tuk-Tuk charging station powered by renewable energy resources such as PV and wind will be more cost-effective and environmentally friendly than a hybrid-DG (Diesel generator) system.
- The developed control and optimisation model will minimise the use of the battery and prolong its life span.
- The proposed standalone off-grid electric Tuk-Tuk charging station powered by renewable energies will be beneficial to a rural population with no grid connection.

1.8 Publications during the study

L. Bokopane, K. Kusakana and H. J. Vermaak (2014, Nov.). "Hybrid system configurations and charging strategies for isolated electric Tuk-Tuk charging station in South Africa" *International Journal of Electrical Engineering*, *Volume 8* (11), pp. 1517-1522.

L. Bokopane, K. Kusakana and H. J. Vermaak (2015, Mar.). "Optimal energy management of an isolated electric Tuk-Tuk charging station powered by hybrid renewable systems" *International Conference on the Domestic Use of Energy (DUE)*, pp. 193-201.

1.9 Dissertation layout

This dissertation has been organised into seven Chapters, with the main research results being presented in Chapter IV, Chapter V and Chapter VI.

Chapter I presents the background of the work, underlines the problems and outlines the objectives and methodology.

Chapter II reviews the state of the electric vehicle; its technologies and its origins; the type of vehicle that needs charging, as well as the type of batteries that are normally used in such a vehicle and determine whether the method of charging ordinary electric vehicles is the same as that of an electric Tuk-Tuk.

Chapter III discusses the methodology that will be used to meet the objectives, and the methodology entails an investigation of the resource assessment per site; a description of the different components that can be incorporated in the architecture of a hybrid system, and its operating principles, charging strategies, vehicle and load analysis.

Chapter IV presents a techno-economic analysis of different feasible supply configurations of the charging station powered with renewable energies, using HOMER software to obtain the simulated results.

Chapter V gives a general overview of the optimisation algorithm design problem which is to maximise the use of the HRES and minimise the use of BESS. The mathematical model of the problem to be solved in this work is formulated. The choice of a suitable optimisation algorithm is discussed.

Chapter VI presents analyses and discusses the results which indicate which charging strategies entail minimal BESS and optimum HRES utilisation, without any load deficit at the charging station.

Finally, **Chapter VII** concludes the work of this thesis and sets the stage for future studies.

Chapter II: Literature review

2.1 Introduction

This chapter looks into the history of electric vehicles, electric vehicle technologies as well as electric vehicle charging stations. It then outlines the electric vehicle chargers and connector standards.

2.2 Electric vehicle technologies

An electric vehicle is defined as an automobile that is propelled by one or more electric motors, using electrical energy stored in batteries or another energy storage device [8]. The rechargeable batteries power the controller which in turn powers the electric motor. The electric vehicle operates on an electric/current principle. It uses a battery pack (batteries) to provide power for the electric motor. The motor then uses the power received from the batteries to rotate a transmission and the transmission turns the wheels [9]. The electric motor, rechargeable battery and controller are the important part of the EV, however for the purpose of this study an emphasis will be on battery as it is the most practical type of technology.

The types of electric vehicle in use today are very different from the first model that was designed back in the 1830's and since then electric vehicles and their technologies have improved dramatically. Table 2.1 below takes us through the years of development and the improvements made by each designer to date.

Table 2.1: Brief history of electric vehicles [8]

1832–1839	Robert Anderson, of Scotland, builds the first prototype electric-powered carriage.
1935	Thomas Davenport, of the United States (US), invents and installs the first direct current electrical motor in a car that operates on a circular electrified track.
1888	German engineer Andreas Flocken builds the first four-wheeled electric car.
1891	William Morris of Des Moines, Lowa, builds the first successful electric automobile in the United states.
1897	The first commercial electric vehicles enter the New York City taxi fleet. The carmaker, Pope Manufacturing Co., becomes the first large-scale EV manufacturer in the US. In 1899 The "La Jamais Contente," built in France, becomes the first electric vehicle to travel over 100 km per hour.
1900	Electricity-powered cars become the top-selling road vehicle in the United States, capturing 28% of the market.
1912	The electric starter, invented by Charles Kettering, obviates the need for the hand-crank, making it easier for more people to drive petrol-powered cars.
1947	Oil rationing in Japan leads carmaker Tama to release a 4.5 hp (746 × 4.5 watts) electric car with a 40V lead acid battery.
1972	Victor Wouk builds the first full-powered, full scale hybrid vehicle.
1976	France's government launches the "PREDIT" programme accelerating EV RD&D. In 1996, to comply with California's Zero Emission Vehicle (ZEV) requirements of 1990, General Motors produces and begins leasing the EV1 electric car.
1997	In Japan, Toyota begins sales of the Prius, the world's first commercial hybrid car. 18,000 are sold in the first production year.
2010	The BEV Nissan LEAF is launched.
2011	Nissan LEAF wins European Car of the Year award.
2012	Deliveries of its sibling, the Opel Ampera, begin in Europe in February 2012.
2013	As of July 2013, the Renault–Nissan Alliance is the world's leading plug-in electric vehicle manufacturer with global sales of 100,000 all-electric units delivered since December 2010.

To date we have different types of electric vehicles, namely the battery electric vehicles, plugin hybrids electric vehicles, extended- range electric vehicles, electric Tuk-Tuks as well as neighbourhood electric vehicles, and they all have different internal combustion and different applications and a common aspect of charging which are explained in details in Table 2.2 below.

Table 2.2: Types of Electric vehicles [10]

Battery Electric Vehicles	Electric vehicles (EVs) use electric motors instead of an internal combustion engine (ICE) to propel a vehicle. The electric power is derived from a battery of one of several chemistries including lead acid, nickel metal hydride (NiMH) and lithium-ion (Li-ion).
Plug-in Hybrid Electric Vehicle (PHEVs):	A plug-in hybrid electric vehicle (PHEV) has an internal combustion engine (ICE) with a motor along with a battery connected in parallel to the ICE. Such vehicles are generally regarded as full hybrids with bigger motor/battery and a plug to recharge.
Extended-range EVs (E-REVs):	These vehicles have an internal combustion engine (ICE) or other secondary source connected in a series configuration to a generator to supply the batteries. The drive range and speeds are comparable to ICE vehicles.
Electric Tuk-Tuk (ETT's):	An Electric Tuk-Tuk (ETT) is an electric vehicle that uses the same concept of charging as the traditional EV, with a speed of 50 km/h and a weight of 200 – 400kg.
Neighbourhood Electric Vehicle	(NEV) is a U.S. denomination for battery electric vehicles that are legally limited to roads with posted speed limits as high as 45 miles per hour (72 km/h) depending on the particular laws of the state, they are usually built to have a top speed of 30 miles per hour (48 km/h), and have a maximum loaded weight of 3,000 lb. (1,400 kg).

The battery selection process depends upon what the designer intends to accomplish in his design. There are different types of batteries to date which possesses different behaviour and performance criteria. These performance criteria include specific power, typical voltage, amp hour efficiency, energy efficiency, commercial availability, cost, operating temperatures, self-discharge rates, number of life cycles and recharge rates [11]. Table 2.3 discusses different battery types that could potentially be used as part of the propulsion system in electric vehicles.

Table 2.3: Types of Electric vehicle batteries [11]

Batteries	**Their uses**
Lead-acid	Lead acid batteries are widely used for starting ICE vehicles, However for EVs, more robust lead acid batteries that withstand deep cycling and use gel rather than liquid electrolyte are used. These batteries are more expensive to produce.
Nickel Cadmium	The nickel cadmium (NiCad) battery was considered to be one of the main competitors of the lead acid battery for use in EVs, as it has nearly twice the specific energy of lead acid batteries. It has high specific power, a long life cycle, low self-discharge, good long-term storage and a wide range of operating temperatures. Its disadvantages include low operating voltage, high investment costs and environmental hazards.
Nickel-metal hydride	Nickel-metal hydride batteries have a much longer life cycle than lead-acid batteries and are safe and abuse tolerant. These batteries have been used successfully in all-electric vehicles and are widely used in hybrid electric vehicles. Of all the new battery systems NiMH is considered to be one of the most advanced and has been used in a range of vehicles, including the Toyota Prius.
Lithium-ion	Lithium-ion batteries have a high power-to-weight ratio, high energy efficiency, good high-temperature performance, and low self-discharge. These batteries are more expensive than NiCad and they need protective circuits to limit peak voltages.
Ultra capacitors	Ultra capacitors can provide vehicles with additional power during acceleration and hill climbing and help to recover braking energy. They may also be useful as secondary energy-storage devices in electric drive vehicles because they help electrochemical batteries, level load power.

This part of the study focuses primarily on the views of previous researchers with regards to the electric vehicle technologies.

Wang et al [12] presented a paper on the key technologies of lithium batteries for electric vehicles. Relative to the main problems faced by the electric vehicles using lithium batteries in the application process, the paper studied the lithium battery's safety and consistency. The paper introduced the lithium battery material, its manufacturing technologies, the battery management system as well as the battery performance platforms.

Yui [13] provided an overview on battery technology for electric vehicles and other industrial projects. Through an overview of real-life applications, the advantages and disadvantages of various battery technologies and chemistries were discussed as well as the capabilities of batteries and the common misunderstanding of batteries.

Chan [14] provided an overview on the current status and future trends in electric vehicle technology. The emphasis was on the impact of rapid development of electric motors, power electronics, microelectronics and new materials. Comparisons were made among various electric drive systems and battery systems. The market size of electric vehicles in the coming years and the potential electric vehicle impacts were also discussed.

Chan and Wong [15] presented a review on the electric vehicle technology's state of the art. The paper reviewed the status of the electric vehicle and the hybrid electric vehicle's state of the art, which placed an emphasis on the engineering philosophy and key technologies. They also addressed the importance of the integration of technologies of the automobile, electric motor drive, electronics, energy storage, controls, and the importance of integrating society strength from the government, industry, research institutions, electric power utilities and transportation authorities. They also discussed the challenges of EV commercialisation.

Maggeto [16] provided an overview of Electric vehicle technology: a worldwide perspective. He discussed the existing EV and HEV technology and the challenges associated with creating a market for this type of vehicle. According to his study, the demand of research development and design effort in the field of drives and charging infrastructure could become enormous and a challenging field for the European Power Electronics and Drivers Community.

2.3 Electric vehicle charging station infrastructure

An electric vehicle charging station, also called an electric recharging point, charging point and Electric vehicle supply equipment (EVSE), is an element in an infrastructure that supplies electric energy for the recharging of plug-in electric vehicles, including all-electric cars, neighbourhood electric vehicles and plug-in hybrids [17].

An electric vehicle charging station acts as the point of transfer from the charging point to the vehicle. There are different categories of recharging the EV's battery in charging stations, which are in line with the charging levels, different modes, a description of the types of charging as well as charging times and these are explained in this chapter [17].

There are several operational charging stations in use presently, and for the purpose of this study emphasis will be placed on the off-grid type which is powered by renewable energies. The different types of EVCS are summarised and categorised below:

2.3.1 Hybrid electric vehicle charging station powered by photovoltaic and wind energy

This type of charging stations incorporates renewable energies that comprise of solar panels, wind turbines as well back up batteries to store excess energy.

Lukic et al [18] investigated the use of all-electric auto rickshaws for transportation in Asia. The all-electric vehicle was designed and tested, and a model of the vehicle was developed for use in system level simulations. In addition, they also presented the operation of the entire transportation infrastructure including an off-grid recharging "mother" station. Their research showed that the mother station with a 480kW PV, 358kW wind turbine, and 350kW propane generator would able to power up to 600 auto rickshaws. 61% of the energy that was used for recharging this vehicle was obtained from renewable resources whilst 39% came from the generator.

Kusakana and Vermaak [19] discussed the possibilities of using electric Tuk-Tuk battery charging stations in the rural areas of the Democratic Republic of Congo (DRC); the basic specifications of the proposed vehicle propulsion system were taken into account. Their proposed charging station would be powered by a renewable energy source such as wind or photovoltaic (PV) in a standalone or in hybrid configuration with a battery storage system to avoid the use of diesel generators or additional stresses on the very weak electrical grid, where available. They simulated different feasible configurations of the charging station using renewable energies with the aid of HOMER software and then compared the results to the corresponding diesel generator while responding to the battery charging energy requirements of the Tuk-Tuk. To select the best suitable configuration with regard to the equipment setup, energy production, financial viability of the project as well as a prolonged life-span, two different strategies for operating the charging station were used to analyse the results that were simulated.

Bancila et al [20] presented several possibilities for electric power supply from renewable sources of electric vehicle charging stations. The supply system sizing and the economic analysis were performed using Homer energy software and the local resources data needed to optimise the system were taken from the RETScreen databases. In this way they were able to choose the photovoltaic panels depending on the solar radiation, and the wind turbines according to the wind parameters of that particular region. The location chosen for the charging stations was Huşi city, Vaslui County, at an average altitude of 82 m above sea level, accessible from the European road E581. The results obtained with the three systems analysed by Homer simulation showed that the choice of an appropriate power charging station should take into account both the local resources and the policies to use and encourage renewable energy, in order to establish the technical and financial feasibility of the system.

2.3.2 *Electric vehicle charging station powered by photovoltaic energy*

The above-mentioned charging station is comprised only of solar panels and a BESS for energy storage during off-peak hours. The energy used to recharge the EV or ETT is harnessed directly from the sun.

Ingersoll and Perkins [21] presented a photovoltaic charging station for electric vehicles which consisted of a cantilevered steel canopy supporting the 2.1 kW amorphous silicon solar arrays. Their system configuration comprised of seven rows of six PV modules each at a fixed angle of 22.5 degrees facing 40 degrees west of south. The design was optimised with the aid of computer simulations for the local climate because of restrictions in the placement and orientation of the entire facility. The facility was then integrated with the utility grid through the Santa Monica City Hall building and it covered seven parking spaces with an equal number of conductive AC charging ports. A didactic display on solar electricity, electric vehicles as well as a number of permanent monitoring devices made up the educational element of the facility. The output of this station proved to be sufficient to power on an annual basis, four EVs at that time, and in future it would be designed in a manner that would enable it to power up to seven EVs. The modular design of this solar EV charging facility was intended to promote the concept of a residential or commercial refuelling infrastructure for alternative fuel vehicles.

Abella and Chenlo [22] presented a photovoltaic charging station for EVs. Their general objective was to study and promote the use of PV energy to charge EVs in an urban area. Their installation had a 9.24 kW PV generator designed as a curved parking cover with 6 different tilt angles, from 12.5 degrees to 50 degrees. The two electric charging towers where used to manage the system energy flow, user control and system monitoring. Then the two connected invertors where used to feed the energy to the EV and to excess the electrical grid. The installation was designed to be portable for demonstration purposes.

2.3.3 Electric vehicle charging station powered by wind energy

This type of charging station is comprised only of wind turbines, as the energy for recharging EVs and ETTs is generated from the wind with aid of wind turbines energy technologies. Most wind energy technologies can be used as standalone applications or connected to a utility power grid and their literature is summarised in this section.

Muljadi et al [23] explored their idea on one type of wind-powered battery charging. Their paper analysed the properties of the system components. In their study they investigated the effect of parameter variation and the system configuration on the system performance. They presented two basic methods of shaping the torque speed characteristic of the generator. They discussed the uncompensated as well as the compensated systems. They also explored the control strategies to improve system performance.

2.3.4 General overview of an electric vehicle charging station

These chargers are usually classified according to output voltage and the rate at which they can charge a battery and they are subdivided into levels, where Level 1 charging is the slowest, and can be done through most wall outlets at 230 volts and 16 amps AC. Level 2 charging is similar to level 1 and it can be done at semi-public places at 230 volts and 16 amps AC. Level 3 charging is the fastest, and can be done with a power output of greater than 14.4 kW [17]. Table 2.4 below presents an overview on the current state of the types of electric vehicle charging stations.

Table 2.4: An overview of the charging station [10] [17]

	Level 1	**Level 2**	**Level 2 /3**	**Level 4**
Description	Convert AC power to DC high voltage to charge BEV.	Convert AC power to DC high voltage to charge BEV.	Convert AC power to DC high voltage to charge BEV.	High-voltage, high current delivered to the vehicle.
Charging types	Home charging	Semi-public charging	Public charging	DC Fast charging
Power supply	Single phase 3.3 kW 230 VAC/16 A.	Single phase 7.4 kW. 230 VAC/16 A 3-phase 22kW 400 VAC/ 32 A.	Three phase 43 kW 400VAC/63 A.	Direct current 50 kW 400 - 500 VDC 100 - 125 A.
Charging time	6 - 8 hours for a complete charge.	3 - 4 hours for a complete charge.	20 - 30 minutes for a complete charge.	20 – 30 minutes for a complete charge.
Different modes	**Mode 1-** slow charging.	**Mode 2-** slow charging.	**Mode 3-** slow or fast charging.	**Mode 4-** fast charging.

- Level 1 - mode 4 will be used, because it is suitable for the remotes areas not served by the grid and it will therefore be used in this research as a charging option for electric Tuk-Tuks.

2.4 Electric vehicle charging station technologies

Electric vehicle charging station technology basically includes batteries, motors and inverters just to mention a few. Several papers have been published with regards to EVCS technologies and a summary is available in the literature below.

Benzai and Wong [24] presented research done, on electric vehicle charging station technologies. Their proposal regarding smart grid brought new opportunities and challenges for the development of electric vehicle charging station systems. They introduced a domestic and foreign research status concerning electric vehicle charging station. They also discussed the key technologies of electric vehicle charging stations and analysed the direction of electric vehicle charging stations in depth.

Wu et al [25] provided an overview of a highly reliable communication technology in electric vehicle charging stations. They introduced the communication, data collection terminals, data transmission networks and data processing gateway system in EV charging stations. A reliable mechanism which contained redundant sending, local cache and dynamic network organising technologies, were implemented to guarantee the reliability of the communication in an EV charging system. Furthermore, the technology introduced in that paper could also be implemented in other cyber-physic systems to improve communication reliability.

2.5 Electric vehicle charging station battery energy storage system/battery banks

Batteries normally serve two purposes in a charging station - namely battery banks and EV batteries for swapping. Battery banks serve an important role in an electric vehicle charging station, as they can store generated electricity during off-peak hours and electricity can be used when the production of energy is at its lowest or even during unfavourable weather conditions, whilst battery swapping is suitable when fast charging is not available or even when the driver does not have time for charging. Below is a summary of related reviews on battery swapping and on battery banks.

2.5.1 Operational aspects of a battery bank at the charging station

Grau-Unda et al [26] presented a publication on energy storage for balancing a local distribution network area. They demonstrated that the reliable, high-efficient and cost-effective energy storage systems can undoubtedly play a crucial role for a large-scale integration with power systems of the emerging distributed generation and for enabling the starting and the consolidation of the new era of so-called smart grids. They established that a non-exhaustive list of benefits of the energy storage properly located on modern power systems with a distribution grid could be as follows: it could increase voltage control, frequency control and stability of power systems, it could also reduce outages; it could allow the reduction of spinning reserves to meet peak power demands; it could reduce congestion on the transmission and distributions grids, it could release the stored energy when energy is most needed and expensive; it could improve power quality or service reliability for customers with high value processes or critical operations, and so on. The main goal of the book was to give a date overview on: (I) basic and well proven energy storage systems; (II) recent advances on technologies for improving the effectiveness of energy storage devices; (III) practical applications of energy storage, in the emerging era of smart grids.

2.5.2 Operational aspects of battery swapping at the charging station

Battery swapping could very well be the solution for vehicles designed with a swappable battery pack when travelling longer distances, and the literature below touches base on that topic.

Yang et al [27] presented a paper on a dynamic operation model of the battery swapping station for EV in the electricity market. Their paper presented a battery swapping station (BSS) as a new proposed mode of supplying power to the EV. Different from the battery charging station (BCS), the BSS prepares the batteries for EVs in advance and could complete the battery swapping in a short time. The operations designed for the BCS were not appropriate for BSS anymore and the research about BSS was at an early stage. They proposed a dynamic operation model of a BSS in the electricity market. Their model was based on short-term battery management and included the mathematical formulation and market strategy. They tested the model in a 24-hour simulation. The result shows clearly that the BSS makes decisions in a market environment through tracing the number of batteries in different conditions and acquires additional revenue by responding actively to the price fluctuation in the electricity market. The feasibility and the practicability of the model were confirmed.

2.6 Electric vehicle charging station charger and connector standards

For an electric device certain standards have to be set and the same is true for Electric vehicle connectors. Most EVs and EVCS use the Society of Automotive Engineers (SAE) J1772 connector and receptacle that is standard for both level 1 and 2 charging equipment. Standardisation in this area is an on-going issue for DC fast charging. Almost all current DC fast charge EVCS in the US use the CHAdeMO connector, developed in Japan and used by Japanese EVs like the Nissan LEAF and Mitsubishi iMiEV, which allows vehicles to connect to DC fast chargers [28], and the two are reviewed and categorised below.

In previous years quite a number of chargers were developed and adapted. In 2001 SAE J1772 was developed and introduced as a charging interface, but it was only capable of delivering 6.6kW. Later an improvement was made which allowed it (J1772-2009) to deliver up to 19.2 kW via single phase 120-240V AC with currents of up to 80A. However, it is certified as 30A although the standard is written as 80A. Recently a Combo coupler variant of the J1772-2009 connector was introduced with additional pins to accommodate fast DC charging at 200-450 DC voltages and up to 90kW.

Another design is the type 2 VDE_AR-E-2623-2-2, this connector was manufactured and developed as a series of 60309-based by a company called Mennekes. This was enhanced with additional signal pins and it has been in use since the late 1990s. These connectors were used as a replacement connectors for Marechal couplers (MAEVA / 4 pin / 32A) as the standard for electric vehicle charging and they have a single size and layout for currents from 16A single-phase up to 63A three-phase (3.7 kW to 43.5 kW) ,but they do not cover the full range of Mode 3 levels.

Finally there is the famous choice for fast DC charge connector called the Chademo which offers charging in the shortest period when compared to other chargers. The word Chademo is basically taken from the abbreviation Charge De Move which is equivalent to charge for moving. The Chademo range offers charges for up to half an hour and is capable of delivering 62.5 kW of high voltage direct current via a special electrical connector.

All these above-mentioned designs include several levels of shock protection, ensuring the safety of charging even during wet conditions, and the literature below summarises the concept behind the fast DC charger.

2.6.1 EVCS connector standards

Liu and Cheng [29] presented a review of international charging coupler standards and their availability. In their paper they presented a study of several worldwide-adopted charging coupler standards and indicate how these standards could enhance unity, safety and compatibility for today's rapidly developing EV charging utilities. Comparisons among the standards were then made regarding their appearance, rated charging voltage, current, communications protocol, proximity and compatible charging standards. Finally, an overview of the currently-available Hong Kong charging stations showed the adaptability of the standardised coupler when connected to local charging stations.

Chen et al [30] presented a standardisation progress investigation on Electric Vehicle Infrastructure in China. They comprehensively presented the standard system of EV charging infrastructure in China and also summarised the general requirements specified by national, industrial and enterprise standards, to compare the differences between IEC, SAE and Chademo standards, and they also discussed the standardisation processes to facilitate vehicle-to-grid (V2G) applications in the near future.

2.6.2 EV battery charger

Electric vehicle chargers are usually vehicle charging points or connection points into which a vehicle can be plugged for charging of its depleted battery, and these points play an important role/part in the infrastructure of EVCS. The literature below explains the basic concept of battery chargers and then presents the research on fast charging.

The charging protocol depends on the size and type of the battery being charged. Some battery types have high tolerance for overcharging and can be recharged by connection to a constant voltage source or a constant current source. Simple chargers of this type require manual disconnection at the end of the charge cycle, or may have a timer to cut off charging current at a fixed time [31].

Bertoluzzo et al [28] presented an overview on battery chargers for plug-in electric vehicles. They dealt with battery chargers for plug-in electric vehicles (PEVs). They described conventional battery chargers based on front-end diode rectifiers, dwelling on the topologies that improve their power factor. Then the bidirectional battery chargers were illustrated, highlighting their capabilities both to achieve a power factor closer to one and to execute vehicle-to-grid services. Finally, they presented the so-called integral battery chargers, showing that they were a viable solution to reduce the power electronics on board the PEVs.

Yilzman and Krein [32] presented a review of battery charger topologies, charging power levels, and infrastructure for plug-in electric and hybrid vehicles. Their review dealt with the current status and implementation of battery chargers, charging power levels, and infrastructure for plug-in electric vehicles and hybrids. Charger systems were categorised into off-board and on-board types with unidirectional or bidirectional power flow. Unidirectional charging limits hardware requirements and simplifies interconnection issues. Bidirectional charging supports battery energy injection back to the grid. Typical on-board chargers restrict power because of weight, space and cost constraints. They could be integrated with the electric drive to avoid those problems. The availability of charging infrastructure reduces on-board energy storage requirements and costs. On-board charger systems could be conductive or inductive. An off-board charger could be designed for high charging rates and would be less constrained by size and weight. Level 1 (convenience), Level 2 (primary), and Level 3 (fast) power levels were discussed. Future aspects such as roadbed charging were also presented. Various power level chargers and infrastructure configurations were presented, compared, and evaluated based on amount of power, charging time and location, cost, equipment, and other factors.

Collin et al [33] presented a paper on the modelling of electric vehicle chargers for power system analysis. They presented simple equivalent models of EV chargers, based on the measurements of a range of actual EVs. Their developed models of the EV chargers were capable of correctly reproducing instantaneous input current waveforms, retaining all relevant electrical characteristics, including harmonic content. In order to make an analysis on the effects of increased penetrations of EV chargers on a low-voltage network, the developed EV charger models were combined with the models of existing loads, as a part of the aggregate residential load mix.

2.6.3 Fast DC chargers

The concept of fast charging is seen as a less time consuming method of charging a vehicle in EVCS, as this method of charging provides high voltages and high currents at a very shorter interval when compared to other forms of charging.

Mauri and Valsecchi [34] presented a paper that investigates the potential impact of fast charging stations on a distribution MV grid and the use of storages to shave peak power demand and provide additional network services.

Trabue et al [35] presented a paper on an electric vehicle DC charger integrated within a photovoltaic power system. They presented a system in which a bidirectional, highly efficient, DC-DC EV charger was placed between the high-voltage DC bus of a PV system and the EV battery. In addition to providing fast charging for the EV battery from PV or from the grid, the charger was capable of diverting fast changes in PV power output to the battery, thereby reducing the rate of change of inverter output power to a level below the ramp rate of existing grid resources. They addressed the sizing of the charger and energy storage based on the PV system rating, the desired maximum ramp rate, and site insulation characteristics. Analysis suggested that small amounts of energy storage could accomplish large reductions in output power ramp rate. Experimental results were shown for a 10 kW, 98% efficient DC-DC charger based on bidirectional four-phase zero-voltage-switching converter.

Kuperman et al [36] provided an overview of a high power Li-Ion battery charger for electric vehicles. The manuscript presented a 50 kW vehicle battery fast charger prototype design. The charger was basically a two-stage controlled rectifier with power factor correction. The input stage consisted of a three phase full bridge rectifier combined with a shunt active power filter.

The input stage was said to have created an uncontrolled pulsating DC bus while complying with the grid codes by regulating the total harmonic distortion (THD) and power factor according to the permissible limits. The output stage was formed by six interleaved parallel groups of two DC-DC converters, fed by the uncontrolled DC bus and performing the charging process. Two independent control boards were employed: active filter control circuitry and the DC-DC control circuitry. The former was operated according to the predetermined grid interfacing behaviour, while the operation of the latter was dictated by the requests from the Battery Management System (BMS). The charger was capable of operating in any of the two typical charging modes: constant current and constant voltage. Control loops were briefly explained throughout the paper and extended simulation/experimental results were presented.

Shi et al [37] studied the dynamic impacts of fast-charging process of battery stacks in the EVs on the active distribution networks with the integration of medium-scale wind energy systems. They proposed the fast-charging model of battery stacks for dynamic stability analysis. They designed the control strategies for this insulated gate bipolar transistor-based (IGBT) AC-DC rectifier and DC-DC converter in the charging stations to meet the requirements during the fast-charging process of battery stacks.

2.7 Conclusion and Future work

Most published studies tend to focus on a renewable energy charging station as a secondary charging option, with the primary option being an overnight charging at home, and this type of charging station is usually situated in metropolitan areas where electricity is readily available. Little attention is paid to off-grid standalone hybrid charging stations in rural areas with poor or non-existent grid connection where the technology of an electric vehicle charging station and its developed standards are not readily applicable.

More research could be conducted on the following topic(s):

- Off grid, standalone hybrid electric Tuk-Tuk charging stations in rural areas powered by renewable energies.
- Optimal battery management and the power flow between the renewable energy resources and the battery to cater sufficiently for the load demand in off-grid isolated standalone hybrid electric Tuk-Tuk charging stations in rural areas powered by renewable energies.

Chapter III: Hybrid system operating principle and resource assessment

3.1 Introduction

This chapter scrutinises the renewable energy potential in the identified locations, to achieve the objectives of this study. This investigation will entail the following: resource assessment to evaluate the potential of resources at different sites as well as the vehicle and load analysis, so as to have an understating of how much energy could be produced using renewable energies (PV and wind) with the rural areas, and isolated islands of South Africa's weather conditions in mind, to fully charge a single Tuk-Tuk and to have a daily estimation of how much energy should be produced to cater for the charging demands. Different charging strategies will be evaluated as will be the operating principle of the hybrid energy system.

3.2Resource assessment

This is one of the most important sections of this chapter; analysing the availability of the resource serves the vital purpose of determining how much energy could be harnessed at a certain location/site, and then having a system in place that would be able to satisfy the load demand. The resources that are under scrutiny in this section are wind and solar and both are discussed in details below:

3.2.1 *Solar*

With regards to solar irradiation it has been said that most areas in South Africa average more than 2 500 hours of sunshine per year, and that the average solar radiation levels range between 4.5 and 6.5 kWh/m^2 in one day. The southern African region, and in fact the whole of Africa, has sunshine all year round [38]. The deserts of Africa, the Sahara, Namib Desert and the Arabian Peninsula, are among the places with highest irradiation on earth, especially 1000km south of the Mediterranean where the annual global irradiation is about twice that of Southern Germany [39]. The annual 24-hour global solar radiation average is about 220 W/m^2 for South Africa compared to about 150 W/m^2 for parts of the USA, and about 100 W/m^2 for Europe and the United Kingdom [40]. This makes South Africa's solar resource one of the highest in the world. The use of solar energy is the most readily accessible resource in South Africa, and Figure 3.1 below illustrates the country's solar irradiation potential.

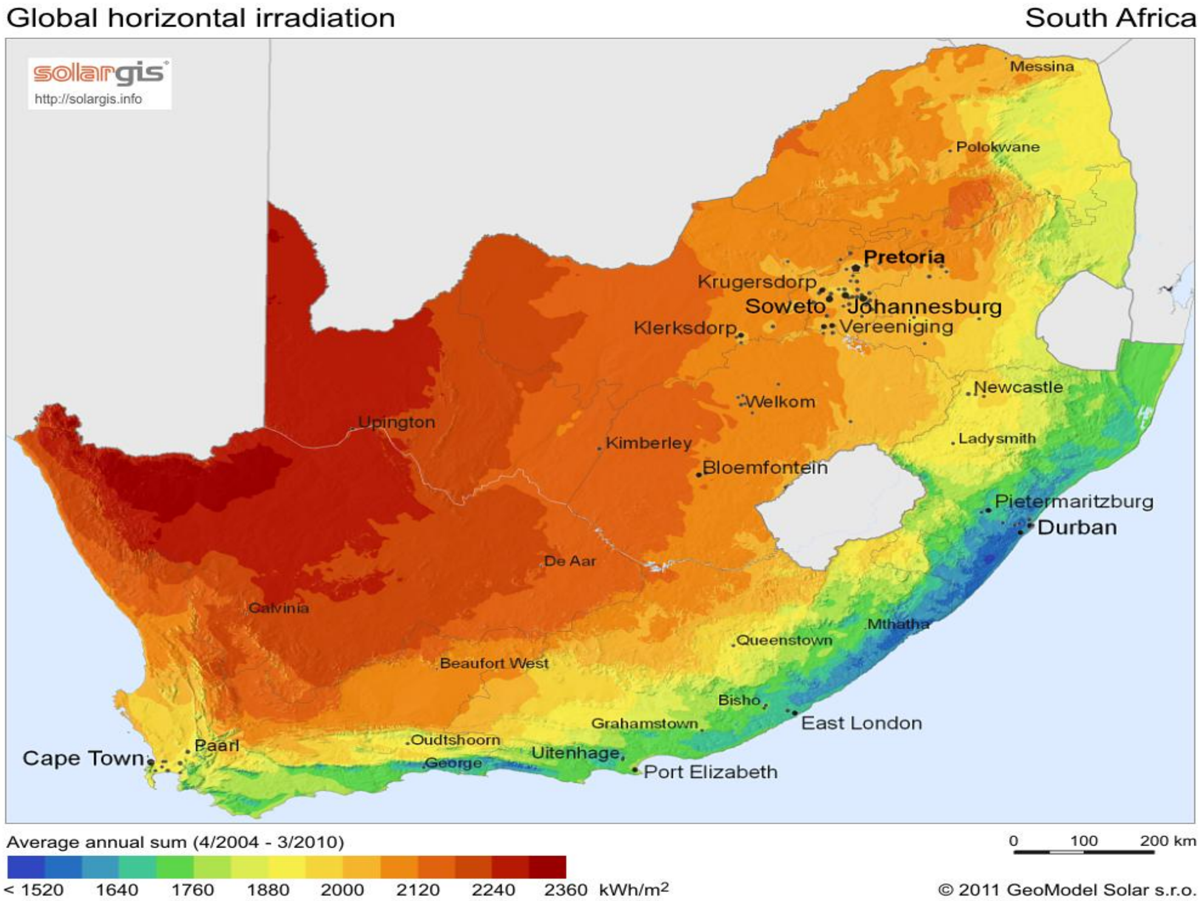

Figure 3.1: Solar energy resources assessment map in South Africa [41]

3.2.2 *Wind potential*

It has been proven through research that the country's coastal areas and the Drakensburg escarpment show the greatest potential for wind energy. The amount of energy that can be extracted from the wind depends on its speed, so the higher the wind speed; the more energy can be harnessed to generate electricity on a large scale [40]. Figure 3.2 illustrates the wind energy potential in the coastal part of the country.

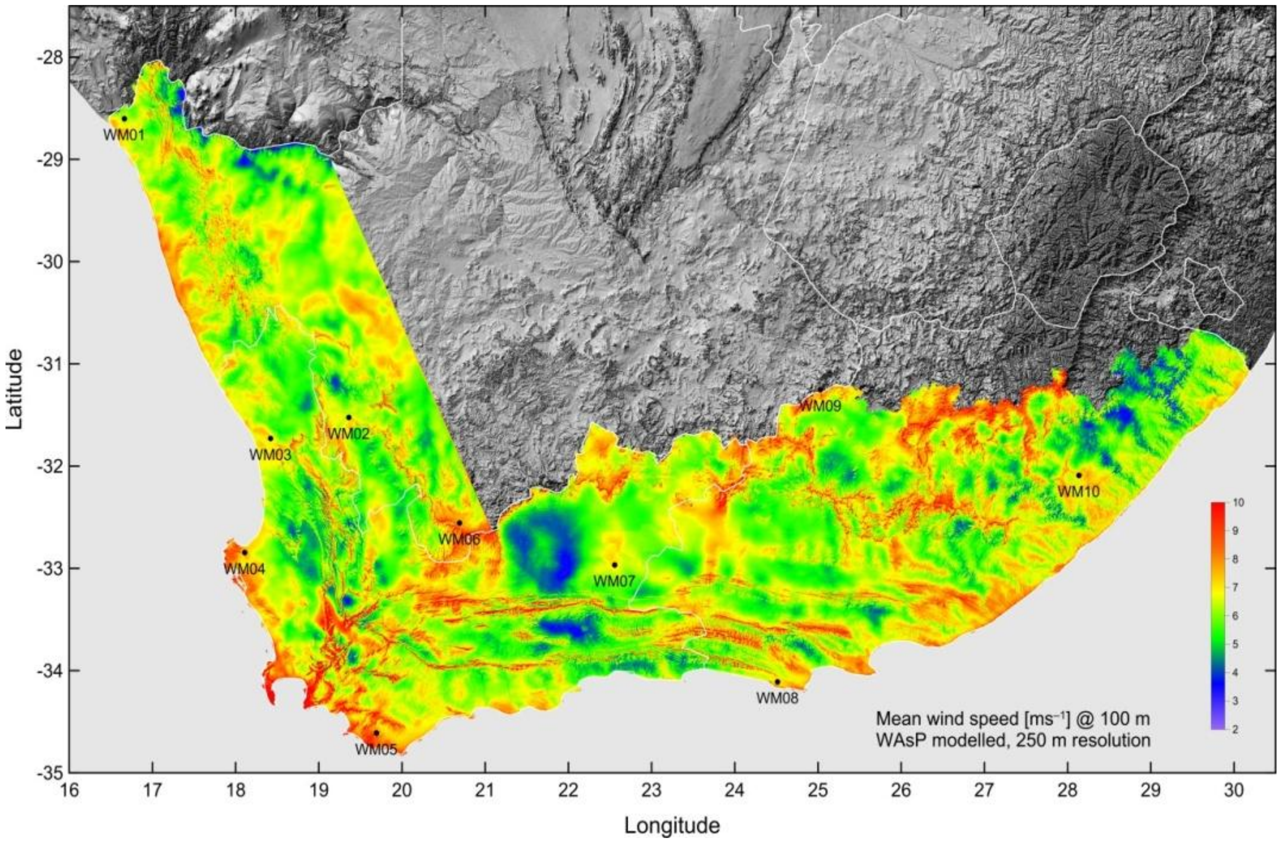

Figure 3.2: Wind energy resources assessment map in South Africa [42]

3.3Investigation of resource assessment per site

A thorough investigation of the potential of wind and solar resources is done in some part of the country, in the rural areas, and isolated islands of South Africa, where the system could be implemented. For the purpose of this study three sites where chosen, the first site being Upington with the highest solar radiation and low wind speeds; the second being Mthatha which has moderate wind speed and solar radiation, and finally Marion Island which has very high wind speeds and low solar radiation. The purpose of this was to assess which system could work well with either resource and which system would be the best possible configuration at each site. The acquired resource assessment data was taken from RETScreen for both wind speed and solar radiation for the identified sites, and are presented on Table 3.1 below.

Table 3.1: Resource assessment per selected site

	Upington		**Mthatha**		**Marion Island**	
Month	Solar Irradiation ($kWh/m^2/day$)	Wind Speed (m/s)	Solar Irradiation ($kWh/m^2/day$)	Wind Speed (m/s)	Solar Irradiation ($kWh/m^2/day$)	Wind Speed (m/s)
January	7.93	4.1	6.10	4.9	5.12	8.3
February	6.96	4.1	5.64	4.7	4.48	8.2
March	5.95	4.0	4.99	4.6	3.22	8.5
April	4.81	4.3	4.26	4.6	2.02	8.0
May	4.03	4.3	3.63	4.9	1.31	8.8
June	3.63	4.3	3.16	5.3	0.94	9.3
July	3.89	4.5	3.40	5.3	1.11	9.8
August	4.82	4.7	4.17	5.3	1.76	9.2
September	5.78	4.5	5.00	5.4	2.65	9.3
October	6.78	4.5	5.36	5.3	3.80	8.8
November	7.66	4.5	5.97	5.0	4.74	8.4
December	8.21	4.3	6.30	4.7	5.21	8.5
Annual	5.87	4.3	4.83	5.0	3.02	8.8

3.3.1 *Site 1: Upington*

This is one of the hottest places in the country, and it is located in the Northern Cape province of South Africa at 29.1 degrees latitude south and 26.2 degrees longitude east. It is has been noted as being the sunniest location on the planet for three months of the year, from November to January, and the coolest and driest month is said to be July.

3.3.2 Site 2: Mthatha

Mthatha is one of the sites that possess moderate wind and solar irradiation in the country, and it is situated in the Eastern Cape Province at 31.6 degrees latitude south and 28.7 degrees longitude east. It is mostly sunny for three months of the years as well, from November to January, and the coolest an driest months are June and July.

3.3.3 Site 3: Marion Island

Is one of the islands that belongs to South Africa that is primarily used for research purposes, it is about 2100 km from Cape town in the Western Cape Province at 46.9 degrees latitude south and 37.74 degrees longitude east, and it politically forms part of South Africa's Western Cape Province. It is the windiest island of South Africa as it experiences high wind speeds all year round and the sunniest months are from November to January.

3.4 Vehicle load analysis

For efficient and effective charging to take place a proper analysis should be conducted into how much energy is needed to fully charge a single Tuk-Tuk and which charging mode is best suitable. The charging modes were covered in chapter 2 under section 2.3.4 presented in Table 2.4.

3.4.1 *Battery specifications of an Electric Tuk-Tuk*

The battery specification in this instance would give a clear indication of the load size of that particular vehicle, and Table 3.2 provides a general description as well as details of the battery parameters. Four 12 volts NiMH batteries will be connected in series to produced 48 volts output to the motors. The selection of the NiMH battery as opposed to its famous competitor, the Li-ion battery, was based on the research output performed on the two types. Research states that Li-ion has a higher specific energy (20% more than that of the NiMH in theory) and output power, however, in practice that is limited at the current development stage. Once the cooling mechanisms of these two batteries are taken into consideration it is noticed that the air cooled NiMH has a higher specific energy at the system level, which optimises its service life, whilst the Li-ion requires powerful cooling structures that contribute via the weight of the coolant, compressor, evaporator and controller, to the system's weight [43].

Table 3.2: Electric Tuk-Tuk battery's general description [44]

Electric system	12 volts DC battery
Nominal Battery Pack Capacity	120 Ah – 130 Ah
Number of Modules per Battery Pack	4 connected in series
DC motor controller	48 volts
Battery Pack Weight (kg)	130 – 160 kg
Nominal Battery Pack Energy (kWh)	5.5 - 6.24

3.4.2 *General load specifications*

Analysing the load to be supplied plays an important role in the deployment of the charging station as this will serve as a reference, when the system is designed, as to how much energy is required to supply the load at hand. Even if the load size is known it is still essential to know how long it will take to fully charge a single Tuk-Tuk and how many kilometres could be travelled after a single charge, this information will be provided by the Tuk-Tuk's general description which is tabulated in Table 3.3 below.

Table 3.3: Electric Tuk-Tuk's general description [45]

Motor of Electric Tuk-Tuk	1000 W / 48 V brush DC motor
Power consumption	6-10 kW /100 km (48V)
Max Speed	30 km/h
Load Capacity	300 kg
Charging time	6-8 h
Charger Capacity	10 A
Recharge time	500 times
Range per charge	100 km-120 km
Net weight of Electric Tuk-Tuk	320 kg

3.5Charging station operation strategies and operating principles

The proposed charging station will be an off-grid type to avoid putting more pressure on the already stressed local grid, and it will incorporate renewable energies that comprise solar panels, wind turbines, a charging point as well as a battery storage system which will be used to store the generated electricity and for battery swapping, as shown in Figure 3.3.

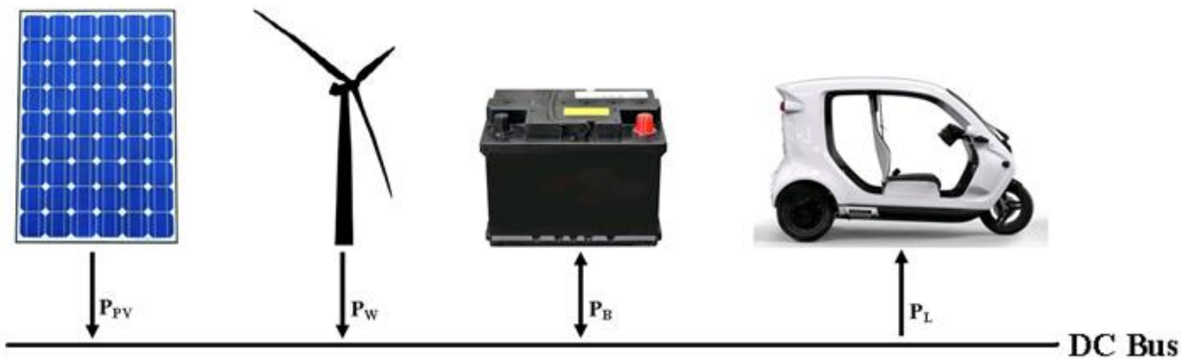

Figure 3.3: System layout of an Electric Tuk-Tuk charging station.

3.5.1 *Scenario1- day charging (S1)*

During the day when there is an abundance of renewable energy resources, charging of an Electric Tuk-Tuk will be done by utilising the resources at the station for 8 hours. During that time both wind and solar energy will be generated throughout the day to cater for the charging requirements at the charging station.

3.5.2 *Scenario 2- night charging (S2)*

During the night when the solar energy is not available, the energy will be provided with aid of the wind system for 8 hours. The wind energy system will be assisted by the battery bank to meet the load demands at the charging station. The energy from the battery bank would have been acquired during off peak hours in the day and also when the generated power exceeds the load.

3.5.3 *Scenario 3- all day charging (S3)*

Charging is provided in three sections for duration of 24 hours, the first being for 8 hours during the early hours of the morning when there is a limited resource of PV and wind energy and charging will be utilised by the minimal availability of renewables and the battery bank. Secondly, there will be charging during day for 8 hours when there is an abundance of both wind and PV, and finally during the night for 8 hours when wind and battery banks are responsible for catering for the load requirement.

3.6 Modelling charging station components

For the purpose of this study only the main components will be taken into consideration, namely solar panels, wind turbines, charging points and battery storage system.

3.6.1 *Solar panels and wind turbine sizing*

The PV and wind energy resources should be sized in such a manner that they would be able to cater for the load demand throughout the year, even during the months with limited resource availability. The size and number of modules of the renewable energy component (wind or Solar) that is needed to produce energy that would insure that load demand is met, regardless of the availability of the resources, are given by equations 3.1 and 3.2 respectively [46]:

$$A_i = \max\left(\frac{E_{load.m}}{E_{i.m}}\right) \quad (3.1)$$

Where A_i is the size of the renewable energy (PV array or wind generator) in m^2; E_{load} is the full load coverage during the worst month in kWh, and $E_{i.m}$ is the energy of the renewable energy (PV and wind) in kWh.

$$N_i = \left(\frac{A_i}{A_{i.u}} \right) \tag{3.2}$$

Where N_i is the actual number of the module of PV array or wind generator, and $A_{i.u}$ is the standard size unit of the renewable energy PV or wind (where the manufacturer standard size unit for PV is $A_{PV.u} = 0.3m^2$ and for the Wind system is $A_{W.u} = 0.65m^2$) [46].

3.6.2 PV system modelling

Usually, in photovoltaic systems, a maximum power point tracking system is used and therefore the PV modules often operate at maximum power. For this purpose, the estimation of maximum power becomes an important parameter in modelling this system component. One of the most known models to describe the maximum output power of the PV module, in MPP conditions is given by [47]:

$$P_m = D_1 G + D_2 T_c + D_3 (\log G)^w + D_4 T_c (\log G)^w \tag{3.3}$$

Where Tc is the junction temperature of PV cells, expressed in degrees Celsius (˚C), and G is the solar irradiance (W/m^2) incident on the modules. The coefficients D_{1-4} and *w* must be determined by fitting the model to experimental data measured in one or more test sites.

T_c can be calculated using the following expression [47]:

$$T_c = T_a + G\left(\frac{NOCT - 20}{800}\right) \tag{3.4}$$

Where T_a is ambient temperature (in ˚C), G is the global solar radiation incident on a horizontal plane (in kW/m^2), *NOCT* is the Normal Operating Cell Temperature.

3.6.3 Wind energy system

The kinetic energy in the wind is a promising source with significant potential in many parts of the world [48]. The wind turbine converts the kinetic energy of wind into mechanical power P_W and then into electrical power. [49]. Different wind generators have different power output performance curves. Therefore, the model used to describe the performance of wind generators is expected to be different [50]. The hourly output power of the wind generator is determined by the average hourly wind speed at the hub height and the output characteristics of the wind generator [51]. Wind velocity at the hub height can be determined by the following expression:

$$v = v_{hr} \times \left(\frac{h}{h_r}\right)^{\gamma} \tag{3.5}$$

Where v is the wind speed velocity at the hub in m/s, v_{hr} is the wind speed at the reference height in m/s, h_r is the height reference in m, h is the hub height in m and γ is the power law exponent.

In function of this wind speed, the model used to calculate the output power, P_W (t) (W), generated by the wind turbine generator is as follows [51]:

$$P_{W(t)} = \begin{cases} a v^3(t) - b.P_R & v_{ci} \angle v \angle v_r \\ P_R & v_r \angle v \angle v_{co} \\ 0 & otherwise \end{cases} \tag{3.6}$$

$$\text{Where } a = \frac{P_R}{v_r^3 - v_{ci}^3} \text{ and } b = \frac{v_{ci}^3}{v_r^3 - v_{ci}^3} \tag{3.7}$$

3.6.4 *Battery energy system modelling*

Modelling the battery is as important as the proposed design (solar-wind renewable energy model), as it determines how efficient the system will operate during unfavourable weather conditions when charging is achieved with the aid of stored energy from the battery banks. Quite a number of researchers came up with different modelling strategies (which include modelling the battery state of charge) to evaluate the battery's reliability as well as its efficiency in the system , (modelling the battery's lifetime) to check how long will the battery be operational in the power system before it needs replacement.

The type of battery that will come into scrutiny here is the NiMH battery as it is the most commonly used battery that is employed in standalone hybrid systems. It has been said that NiMH batteries have high efficiency and, a longer life-span and that is why they are ideal for utilisation in renewable energy systems. Chapter 5 will analyse the battery state of charge of different system configurations and discuss the battery model and battery state of charge under the optimal battery management.

3.7Discussion

Solar energy is only available during the day, and during the night there is a high probability of wind energy. When there is abundance of both or either solar and wind, priority of charging is given to the resources. However when the energy generated at the charging station is less than the load demands, then either resource will be assisted by the battery bank to meet the load. The energy from the battery bank would have been acquired during off-peak hours in the day and also when the generated power exceeds the load requirements.

The charging times depends upon the charging preference (refer to Table 2.4) of the client. When the charging times presented in Table 3.3 is rather inconvenient for the client, then other option of charging such as fast DC charging (mode 4/ level 4) or battery swapping could come into play.

3.8Conclusion

This chapter showcased the potential of renewable energy resources at different sites in the rural areas and isolated islands of South Africa, and presented the load and vehicle analysis so as to provide more insight into how rich the country is in the resources that will be utilised in the charging stations. It also provides a clear picture of how much energy should be available for the purpose of charging a single Tuk-Tuk. Finally, the charging station and different charging times were presented.

Chapter IV: Techno economic analysis

4.1Introduction

The main focus of this chapter is to discuss the various charging strategies that could be implemented to find the best possible configuration of an electric Tuk-Tuk charging station in terms of COE at the rural areas, and isolated islands of South Africa. The charging station is designed, modelled and simulated to evaluate its performance. The techno-economic analysis of different feasible supply configurations of the charging station using renewable energies such as PV, wind and PV + wind, will be simulated using HOMER software.

4.2Charging station components sizing

From chapter III it can be noted that in order to make a selection of a certain components size one needs to apply a mathematical expression, which will serve as a guideline as to which size should be selected to harness energy that would adequately meet the daily demand, even during unfavourable weather conditions. The size and the component cost of main components of the proposed system as well as the load demand by a combination of either component are tabulated in Table 4.1 below. The prices for the PV panels were taken form sustainable.co.za; the batteries were taken from various suppliers on alibaba.com and those of the wind turbines were taken from Bergey wind power turbines. Micro sized wind turbines (1 kW) will be employed due to their cost efficiency.

Table 4.1: Electric Tuk-Tuk charging station's load demand, component sizes and components costs

Load demand per site			**Components size**			**Component cost**		
Day charging	Night charging	All day charging	PV panel	Wind turbines	Single battery	PV panel	Wind turbines	Single battery
5.8 kW	5.8 kW	17.4 kW	1 kW	1 kW, 48 volts	120 Ah, 12 volts	$2500-00	$4500-00	$200-00
				7.5 kW, 48 volts			$268700-00	

4.3Simulated results discussion per site, scenario and system configuration

For this proposed system three scenarios that where discussed in chapter 3 under section 3.5 will be taken into consideration. These scenarios are incorporated into different system configurations under each of the three sites from the rural areas, and isolated islands of South Africa, which possess different resource availability (solar radiation and wind speeds) and from these a mathematical approach as well as a simulation will be performed. The configurations under this study will be the PV system, wind system and PV+ wind system (hybrid), and the focal point of this simulation is to compare all three system configurations during different scenarios to see which combination (system configuration + scenario) is the most cost-effective in terms of COE ($/kWh) that could be produced by that system. The results for each site are tabulated in Table 4.2, 4.3 and 4.4 respectively, and discussed under each table.

4.3.1 Upington results presentation and discussion

Table 4.2 below represents the simulated result of each system configuration (PV, wind & hybrid) and scenario (1, 2 & 3) in Upington.

Table 4.2: Simulation results in Upington

	PV system			Wind system			Hybrid renewable system		
	S1	S2	S3	S1	S2	S3	S1	S2	S3
Initial cost ($)	**4100**	6600	12400	50100	22800	62300	7800	8600	15200
Net present cost ($)	**5649**	13066	23267	71089	32561	88758	10274	15583	25641
Cost of energy ($/kWh)	**0.21**	0.486	0.288	2.646	1.200	1.110	0.382	0.580	0.318
Operational cost ($/year)	**121**	506	850	642	761	2070	194	546	817
Replacement cost ($/year)	**2172**	7709	12806	25253	11688	31798	3353	8065	12241
Number of (1 kW) PV panels per system	**1**	2	4	-	-	-	1	1	3
Number of (1 kW) wind turbines per system	**-**	-	-	9	4	11	1	1	1
Number of batteries per system (Ah)	**8**	8	12	48	24	64	4	8	16

If the PV architecture was to be selected for this location, then the most cost-effective scenario would be scenario 1 where the initial cost for implementing such a project would be $4100 at a net present cost of $5649 with only 0.21 $/kWh, and such a system would comprise a 1 kW PV panel and 8 (12 volts) batteries.

If the wind system was to be considered for this location then the most financially viable option would be scenario 2, with an initial cost of $62300 and a net present cost of $88758, while the cost of energy in would be 1.110 $/kWh, and such a system would comprise 11 wind turbines and 64 (12 volts) batteries.

Where a hybrid (PV + wind) Architecture is considered for this location, then the most reasonable choice would be scenario 1 which has an initial cost of $15200 and a net present cost of $25641, with a cost of energy of only 0.318 $/kWh. Such a system would comprise a 1 kW PV panel and a 1 kW wind turbine and 16 (12 volts) batteries.

From the three mentioned systems and scenarios the overall most cost-effective solution would be scenario 1 with system configuration 1 (PV system).

4.3.2 Mthatha results presentation and discussion

Table 4.3 below represents the simulated result of each system configuration (PV, wind & hybrid) and scenario (1, 2 & 3) in Mthatha.

Table 4.3: Simulation results in Mthatha

	PV system			Wind system			Hybrid renewable system		
	S1	S2	S3	S1	S2	S3	S1	S2	S3
Initial cost ($)	9900	10700	31300	15400	24400	45500	10600	14800	**29500**
Net present cost ($)	12737	16578	41016	22949	34674	53941	15019	22143	**36640**
Cost of energy ($/kWh)	0.474	0.617	0.508	0.854	1.290	0.668	0.559	0.824	**0.454**
Operational cost ($/year)	222	460	760	591	804	660	346	574	**559**
Replacement cost ($/year)	4427	7930	14673	8962	12355	9760	5609	9144	**10163**
Number of (1 kW) PV panels per system	3	3	9	-	-	-	1	3	**5**
Number of (1 kW) wind turbines per system	-	-	-	2	4	7	1	1	**2**
Number of batteries per system (Ah)	12	16	44	28	24	56	16	12	**36**

If a PV architecture was to be selected for this location, then its most viable solution would be scenario 1 which has an initial cost of $9900 with a net present cost of $12737, whilst the cost of energy produced would be 0.474 $/kWh, and such a system would comprise 3 (1 kW) PV panels and 12 (12 volts) batteries.

If a wind system was to be considered, the most cost-effective solution would be scenario 1 with an initial cost of $15400 with a net present cost of $22949, and the cost of energy produced would be 0.854 $/kWh. This type of system would comprise 2 (1 kW) wind turbines and 28 (12 volts) batteries.

If a hybrid (PV + wind) architecture was to be selected for this location, the cheapest solution would be scenario 3, which has an initial cost of $29500 with a net present cost of $36640 and a cost of energy produced of 0.454 $/kWh. This type of system would comprise 5 (1 kW) PV panels, 2 (1 kW) wind turbines and 36 (12 volts) batteries.

Of the three configurations and scenarios in this location, the most cost-effective solution in terms of cost of energy produced in $/kWh, would be scenario 3 of the hybrid system configuration.

4.3.3 Marion Island results presentation and discussion

Table 4.4 below represents the simulated result of each system configuration (PV, wind & hybrid) and scenario (1, 2 & 3) in Marion Island.

Table4.4: Simulation results in Marion Island

	PV system			Wind system			Hybrid renewable system		
	S1	S2	S3	S1	S2	S3	S1	S2	**S3**
Initial cost ($)	24800	28900	97796	7300	8100	21100	9000	9000	**18700**
Net present cost ($)	31159	36807	79500	10773	12176	25924	12213	13687	**23866**
Cost of energy ($/kWh)	1.160	1.370	1.213	0.401	0.453	0.321	0.454	0.509	**0.296**
Operational cost ($/year)	497	619	1431	272	319	377	251	367	**404**
Replacement cost ($/year)	10413	12585	31489	4133	4829	5569	4216	5767	**6349**
Number of (1 kW) PV panels per system	8	9	27	-	-	-	1	1	**1**
Number of (1 kW) wind turbines per system	-	-	-	1	1	8	1	1	**1**
Number of batteries per system (Ah)	24	32	60	12	16	32	8	8	**32**

If a PV architecture was to be selected for this location, the most viable solution would be scenario 1with an initial cost of $24800 and net present cost of $31159, with a cost of energy produced of 1.160 $/kWh. This architecture would comprise 8 (1 kW) PV panels and 24 (12 volts) batteries.

If a wind system was to be considered, the most cost-effective solution would be scenario 1. Initial cost for such a system would be $7300 with a net present cost of $10773, and the cost of energy produced would be 0.401 $/kWh. This architecture comprises 1 (1 kW) wind turbines and 16 (12 volts) batteries.

If a hybrid (PV+ wind) architecture was to be selected for this location, the cheapest solution would be scenario 3, with an initial cost of $18700 with and net present cost of $23866, whilst the cost of energy produced would be 0.296 $/kWh. This architecture would comprise 1(1 kW) PV panels, 2 (1 kW) wind turbines and 32 (12 volts) batteries.

From all three mentioned scenarios and system configurations the most cost effective solution is a scenario 3 in a hybrid architecture, as this is the most cost-effective method in terms of cost of energy produced in $ kWh.

4.4Discussion

The acquired simulation results showcased the effectiveness of the model. The model behaved in accordance with the input data. There are aspects of marginal error that should be taken into account when it comes to the simulated results, this will depend on the method of data collection.

4.5Conclusion

This chapter presented different solution for the design of electric Tuk-Tuk charging stations in two isolated rural areas and one research based island of South Africa. It showcased three different system configurations and scenarios to achieve the same charging strategies from different resource availability. The simulations were performed with aid of HOMER software and three different strategies were used with one resource configuration (*solar or wind*) respectively, and also a hybrid configuration of both solar and wind, and from all systems and scenarios the best solution is then determined in terms of COE produced.

Chapter V: Charging station optimal control and proposed algorithm

5.1Introduction

The main objective of this chapter is to develop a mathematical model for controlling and optimising the daily operation of a standalone hybrid renewable energy system by maximising the usage of the renewable resources, whilst minimising the utilisation of the battery bank for supplying the required energy at an electric Tuk-Tuk charging station without any load rejection. The constraints will be set out in the optimisation problem formulation for the hybrid renewable energy system as well as the operational limits that should be adhered to in the system design stages.

5.2HRES model formulation

5.2.1 Hybrid renewable energy system configuration

The HRES will be configured in a way that it should be able to meet the load demand without any load rejection. Charging will be provided by the power generated from the renewable energy technologies–PV and wind– whilst the battery stores the excess electricity from these resources. The energy that has been stored in the batteries will be used only when the output energy from the PV and wind cannot meet the demand. The configuration for the hybrid renewable energy system is shown in chapter 3 (refer to Figure 3.3). Both the PV system and wind system were covered in chapter 3 under sections 3.6.1 and 3.6.2 respectively.

5.2.2 *Battery system operating points*

A battery is a storage device essential for storing electrical energy for maximum utilisation of intermittent renewable resources [52]. The battery life is known to depend on the number of discharge/charge cycles; the amount of energy used at each cycle (state of charge); operational temperature, and discharge/charge current [53]. The difference between power generated by renewable energy sources (PV and wind) and the power demand, determines whether the battery banks should be charged or discharged [54].

During the charging and discharging processes, the state of charge (SOC) at the hour t should fulfil the constraint based on the models presented [55]. State-of-charge (SOC) measures energy left in a battery, and it is critical for modelling and managing batteries [56]. When the total output power of PV panels and wind generators is greater than the load energy, the battery bank is in charging state. The state of charge of the battery bank at time t can be obtained by [52]:

$$SOC_{(t+1)} = SOC_{(t)} - \frac{\eta_B P_{B(t)}}{E_{BN}} \times t \tag{5.1}$$

Where SOC is the state of charge of the battery; η_B is the battery charging or discharging efficiency; E_{BN} is the battery system nominal energy; P_B is the power flowing from the battery system, and *t* is the sampling time.

5.3 Optimisation problem formulation

5.3.1 Objective function

The objective is to come up with an optimum algorithm design problem to maximise the use of HRES and minimise the use of the battery energy storage system. The objective function can then be subdivided into two sections which are firstly to minimise the usage of BESS, and secondly to maximise the usage of HRES.

$$Min\ f(x) \quad subject\,to \begin{Bmatrix} Cx \leq 0 \\ C_{eq}x = 0 \\ A_x \leq b_{eq} \\ A_{eq}x = b \\ l_b \leq x \leq U_b \end{Bmatrix} \tag{5.2}$$

$$x = f\min con(@of, x_{0,} A, b, A_{eq}, b_{eq}, l_b, U_b.@NL) \tag{5.3}$$

5.3.2 *Fmincon equation solver*

Table 5.1 below represents the function of fmincon used to find the minimum of a proposed problem.

Table 5.1: Fmincon problem solver by objective function and constraints

Objective	Objective function
x_o	Initial point for x
A	Matrix for linear inequality constraints
b	Vector for linear inequality constraints
C	Non-linear inequality constraints
Aeq	Matrix for linear equality constraints
beq	Vector for linear equality constraints
Ceq	Non-linear equality constraints
l_b	Vector of lower bounds
U_b	Vector of upper bounds
NL	Nonlinear constraint function
Solver	'fmincon'
Options	Options created with optimoptions

5.3.3 *Constraints*

Optimal energy flow management among the various energy sources in HRES is necessary since the power output from renewable sources is intermittent and dependent on several uncontrolled conditions [56]. Maintaining a continuous balance between available power and load is mandatory for a stable power system operation [47].

5.3.3.1 Power flow system

The power management strategy (PMS) should determine the power dispatch between the renewable energy sources, the energy storage devices, and the load at the charging station [56], when the total energy generated by the PV and wind generators is greater than the energy required by the load. In this case the energy surplus is stored in the batteries and the controller puts the battery in charge condition. When the battery SOC reaches the maximum value, the control system stops the charging process [56]. When the total PV and wind energy is less than the energy required by the load, the energy deficit is covered by the storage and the controller puts the battery in the discharge condition. If the battery charge decreases to its minimum level, minimum state of charge, the control system disconnects the load there is an energy deficit [57]. Therefore the power balance equality constraint is illustrated here for demand represented as P_L at any interval (t):

$$P_{L(t)} = P_{PV(t)} + P_{W(t)} + P_{B(t)} \tag{5.4}$$

Where $P_{L\,(t)}$ is the load demand at any interval t in kW;

$P_{B\,(t)}$ is the output power of the battery at any interval t in kW;

$P_{PV\,(t)}$ is the output power that is generated from the solar system at any interval t in kW,

and $P_{W\,(t)}$ is the output power produced by the wind energy system at any interval t in kW.

5.3.3.2 Control variable limits

The battery module is modelled as a variable power source controllable in the range of minus rated power, when charging, to its rated power for the 24 hour period [58]. In the HRES the wind energy system and the PV system module are modelled as variable power sources controllable in the range of zero to the maximum available power for a 24 hour period [59]. These are the main component's variable limits at any sampling interval *t*, and they can be expressed as follows:

i. PV energy system,

$$0 \leq P_{PV(t)} \leq P_{PV(t)}^{\max} \tag{5.5}$$

ii. Wind energy system,

$$0 \leq P_{W(t)} \leq P_{W(t)}^{\max} \tag{5.6}$$

iii. Battery energy system.

$$-P_{B(t)}^{rated} \leq P_{B(t)} \leq P_{B(t)}^{rated} \tag{5.7}$$

Where $P_{PV(t)}^{\max}$ is maximum value of the PV system at any interval t;

$P_{W(t)}^{\max}$ is maximum value of the wind system at any interval t;

$P_{B(t)}^{rated}$ And $-P_{B(t)}^{rated}$ are the positive and negative rated powers of the battery system at any interval t.

5.3.3.3 Battery state of charge limits

Battery SOC estimation provides a system operator or control algorithm with knowledge of the available charge remaining in a battery pack [60]. The available battery bank SOC in any sampling interval must not be less than the minimum allowable and must not be higher than the maximum allowable SOC, and these depend on the type of battery used. The battery state of charge at any time t can generally be expressed as [58]:

$$SOC^{\min} \leq SOC_t \leq SOC^{\max} \quad (5.8)$$

The battery SOC will play a pivotal role in prolonging the battery life-span and the following limits should be adhered to, to avoid overload and extreme discharging condition.

i. Maximum state of charge (not more than 95%),

$$SOC_t \leq SOC^{\max} \quad (5.9)$$

ii. Minimum state of charge SOC (not less than 40%).

$$SOC^{\min} \leq SOC_t \quad (5.10)$$

5.3.4 Proposed optimisation algorithm

The objective function of the proposed system is modelled as a non-linear function of the battery output. A MATLAB/fmincon function is designed to find the minimum of a constrained non-linear multi-variable function. It has the ability to solve large-scale programming problems faster, with full constraint support [61]. The constrained non-linear optimization problem can be solved using the "fmincon" solver in MATLAB [61]. The function fmincon of MATLAB is used to solve the problem of the very short-time predictive control [62].

5.4 Optimisation problem solving methods

Over the years a number of researchers have developed different methods of optimisation. Those methods are dynamic programming, fuzzy logic and finally the Quasi-Newton method, and every method is tailored for a specific application. In this section their principles will be explained and the most suitable method for this research study will be selected and justified.

5.4.1 Dynamic programming

Dynamic programming is an optimisation approach that transforms a complex problem into a sequence of simpler problems, and its essential characteristic is the multistage nature of the optimisation procedure and it provides a general framework for analysing many problem types. Within this framework a variety of optimisation techniques can be employed to solve particular aspects of a more general formulation [63].

5.4.2 Quasi-Newton method

The Quasi-Newton (QN) method is used in the optimisation domain for solving a non-linear problem, and its objective is to find a local minimum from the first and second derivative in order to find the stationary point at which the gradient equals zero. fmincon is the default solver for the minimisation of a nonlinear function with non-linear constraints and it is included in MATLAB Toolbox using the QN method [64].

5.4.3 Fuzzy logic

A fuzzy set is a class of objects with a continuum of grades of membership. Such a set is characterised by a membership (characteristic) function which assigns to each object a grade of membership ranging between zero and one. The notions of inclusion, union, intersection, complement, relation, convexity, etc., are extended to such sets, and various properties of these notions in the context of fuzzy sets are established. In particular, a separation theorem for convex fuzzy sets is proved without requiring that the fuzzy sets be disjointed [65].

5.4.4 Proposed optimisation solver

Dynamic programming is excellent for solving optimisation problems however it does not work well on non-linear objects, and it is said to be often nontrivial to write codes that evaluates the sub problems in the most efficient order. Fuzzy logic method can be applied to multi objective optimisation problem, and it is designed to represent uncertain and vague data however it requires more fine tuning and simulation before it is operational. Quasi-Newton method fmincon was selected due to the fact that it is a default solver for the minimisation of a non-linear function with non-linear constraints.

5.4.5 *Discretisation principle*

Analytical methods are best used in optimal operation control problems where both the objective function and constraint models are time dependent. However in a complex equation like this one the load varies with time and the utilisation of the battery largely depends on the load demand as well as the generated power from the renewable energy resources. In this instance a discretisation method can be employed whereby the energy at the station can be sampled in time "N" with a change in time "Δt". For the purpose of this research the sampling time will then be taken as (N = 2). The optimisation toolbox that will be used to solve the formulated problem is fmincon in the MATLAB program, the code under development, will comprise only the variable of "*x*". A MATLAB/fmincon function is chosen because it is designed to find the minimum of a constrained non-linear multi-variable function and it has the ability to solve large-scale programming problems faster, with full constraint support, where the P_{PV}, P_W and P_B will expressed as the functions of "*x*". Mathematical representation of the above-mentioned is as follows:

$$P_{PV} = P_1 = x(1:N) = [x_1, x_2] \tag{5.11}$$

$$P_W = P_2 = x(N+1:2N) = [x_3, x_4] \tag{5.12}$$

$$P_B = P_3 = x(2N+1:3N) = [x_5, x_6] \tag{5.13}$$

5.4.6 *Constraints definition in fmincon syntax*

- Power balance

When the total PV and wind generator power is less than the power required by the load, the energy deficit is covered by the storage and the controller puts the battery in the discharge condition. If the battery charge decreases to its minimum level, minimum state of charge, the control system disconnects the load and there is an energy deficit situation [55]. Therefore the power balance equality constraint is illustrated here for demand represented as P_L at any interval (j):

$$P_{PV(j)} + P_{W(j)} + P_{Bat(j)} = P_{L(j)} \tag{5.14}$$

From the discretisation Figure 5.2 below where N = 2, the power balance can be developed for these two sampling intervals as:

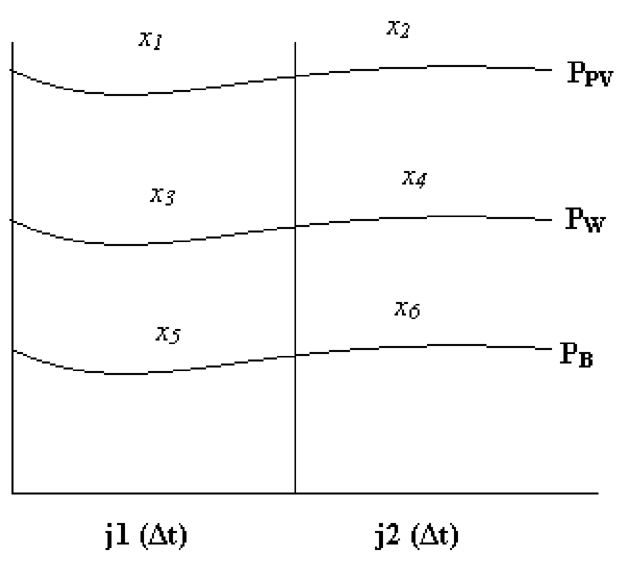

Figure 5.1: Discretisation graph

For $j = 1 \rightarrow x + x_3 + x_5 = P_{L1}$ (5.15)

$$j = 2 \rightarrow x_2 + x_4 + x_6 = P_{L2} \quad (5.16)$$

Taking the coefficient of the equations, the system can be rewritten in a matrix form as:

$$\begin{pmatrix} 101010 \\ 010101 \end{pmatrix} \begin{pmatrix} x_1 \\ x_2 \end{pmatrix} = \begin{pmatrix} P_{L1} \\ P_{L2} \end{pmatrix} \quad (5.17)$$

Using the canonical formulation of the linear equality constraints in fmincon, the power balance can be finally expressed as:

$$Aeq = [eye(N,N), eye(N,N), eye(N,N)] \quad (5.18)$$

$$beq = PL(1:N) \quad (5.19)$$

- Boundaries

The change of minimum values that each power source can produce in different time intervals is "zero"; however, for the specific case of the battery system, this value "$-P_B^{rated}$" is the maximum power entering the battery while charging. The system's lower bounds change can be expressed in vector forms as follows:

$$lb = [zeros(N,1), zeros(N,1), -P_{B\_max} * ones(N,1)] \quad (5.20)$$

The change of maximum values that each renewable source can produce in different time intervals is "$P_{i(j)}^{\max}$", which depends on the availability of the renewable resources. However, for the specific case of the battery system, these values are their maximum rated values "P_B^{rated}" respectively. The system's lower bounds change can be expressed in vector forms as follows:

$$ub = [P_{PV\_\max}(1:N), P_{W\_\max}(1:N), P_{B\_\max}(1:N) * ones(N,1)] \tag{5.21}$$

- Battery dynamic

In this section the operating limits of the battery are represented by the generated power from HRES and the load power, and it can be mathematically expressed as:

$$SOC_{(j+1)} = SOC_j - t\frac{\eta_B}{E_n} \times P_{B(j)} \tag{5.22}$$

Where E_n is the nominal energy from the battery system, and

η_B is the efficiency of the battery system.

This expression can be re-written as:

$$SOC_{(j+1)} = SOC_j - K \times P_{B(j)} \tag{5.23}$$

Proceeding by recurrence, Eq. (*) can be developed as:

For $j = 1 \rightarrow SOC_{(2)} = SOC_1 - K \times P_{B(1)}$ (5.24)

$$j = 2 \rightarrow SOC_{(3)} = SOC_2 - K \times P_{B(2)} \tag{5.25}$$

$$j = j \rightarrow SOC_{(j)} = SOC_1 - K \times \sum_{i=1}^{j} P_{B(j)} \tag{5.26}$$

Replacing Eq. (5.26) into the battery state of charge limit equation and introducing the initial battery state of charge, Eq. (5.8) can be developed as:

$$SOC^{\min} \leq SOC_0 - K \times \sum_{i=0}^{j-1} P_{B(j)} \leq SOC^{\max} \text{ Or} \tag{5.27}$$

$$SOC^{\min} \leq SOC_0 - K \times \sum_{i=1}^{j} P_{B(j)} \leq SOC^{\max} \tag{5.28}$$

The linear inequality equation can then be split into minimum and maximum.

- Maximum inequality:

$$SOC_0 - K \times \sum_{i=1}^{j} P_{B(j)} \leq SOC^{\max} \tag{5.29}$$

$$\text{For } \begin{array}{l} j = 1 \rightarrow SOC_0 - K \times x_5 \leq SOC^{\max} \\ \rightarrow K \times x_5 \leq SOC^{\max} - SOC_0 \end{array} \tag{5.30}$$

$$j = 2 \rightarrow SOC_0 - K \times (x_5 + x_6) \leq SOC^{max}$$
$$\rightarrow K \times (x_5 + x_6) \leq SOC^{max} - SOC_0 \quad (5.31)$$

- Minimum inequality:

$$SOC^{min} \leq SOC_0 - K \times \sum_{i=1}^{j} P_{B(j)} \quad (5.32)$$

For
$$j = 1 \rightarrow SOC^{min} \leq SOC_0 - K \times x_5$$
$$\rightarrow K \times x_5 \leq SOC_0 - SOC^{min} \quad (5.33)$$

$$j = 2 \rightarrow SOC^{min} \leq SOC_0 - K \times (x_5 + x_6) \rightarrow$$
$$K \times (x_5 + x_6) \leq SOC_0 - SOC^{min} \quad (5.34)$$

The linear inequalities from the above equations can now be grouped together as follow:

$$-K \times x_5 \leq SOC^{max} - SOC_0 \quad (5.35)$$

$$-K \times (x_5 + x_6) \leq SOC^{max} - SOC_0 \quad (5.36)$$

$$K \times x_5 \leq SOC_0 - SOC^{min} \quad (5.37)$$

$$K \times (x_5 + x_6) \leq SOC_0 - SOC^{min} \quad (5.38)$$

A matrix form representation of the coefficient of the equations of both the maximum and minimum battery state of charge is as follow:

$$\begin{pmatrix} 0 & 0 & 0 & 0 & -K & 0 \\ 0 & 0 & 0 & 0 & 0 & -K \\ 0 & 0 & 0 & 0 & K & 0 \\ 0 & 0 & 0 & 0 & K & K \end{pmatrix} \begin{pmatrix} x_1 \\ x_2 \\ x_3 \\ x_4 \\ x_5 \\ x_6 \end{pmatrix} \leq \begin{pmatrix} SOC^{\max} - SOC_0 \\ SOC^{\max} - SOC_0 \\ SOC_0 - SOC^{\min} \\ SOC_0 - SOC^{\min} \end{pmatrix} \tag{5.39}$$

This is then the expression of a canonical formulation of the linear inequality constraints in fmincon, and it can be represented in the following manner:

$$A_1 = [zeros(N,N), zeros(N,N), -K * tril(ones(N,N))] \tag{5.40}$$

$$A_2 = [zeros(N,N), zeros(N,N), K * tril(ones(N,N))] \tag{5.41}$$

$$A = [A_1; A_2] \tag{5.42}$$

$$b_1 = (SOC\_\max - SOC_0) * ones(N,1) \tag{5.43}$$

$$b_1 = (SOC_0 - SOC\_\min) * ones(N,1) \tag{5.44}$$

$$b = [b_1, b_2] \tag{5.45}$$

5.5Discussion

The aim of the proposed model is to insure that the HRES is utilised to its maximum capability to meet the load demand, and to minimise the charging/discharging cycle of the battery. In this chapter the constraints that should be adhered to when it comes to the battery state of charge were also presented. The battery should not exceed its discharging/charging capacity. In grid connected HRES charging station when the battery reaches its maximum charging capacity it is disconnected from the supply and the grid is utilised as the energy storage unit. However, the proposed charging station is an isolated off-grid type. In this case when the battery reaches its maximum charging capacity the excess energy will then be dissipated in a dummy load resistive load or static switches (the most cost effective dummy load is the resistive load).

5.6 Conclusion

The mathematical model for controlling and optimising the daily operation of a standalone hybrid renewable energy system was presented. The constraints as well as the optimisation problem formulation for the hybrid renewable energy battery integrated system of 24 hour period were derived by fmincon solver for simulation.

Chapter VI: Simulation results and discussion

6.1 Introduction

In this chapter the model that was developed in the previous chapter is used to ensure that the energy stored in the battery banks is utilised as a last resort when there is a deficit in the HRES at the charging station. The simulations are performed by using fmincon in a MATLAB environment. The results will then be presented, compared and analysed in order to select the best possible system configuration that offers minimal battery usage and maximum usage of the HRES.

6.2 Case studies

A single site (Upington in the Northern Cape Province) exhibiting two different resources availability (a single day in winter and in summer) was selected to investigate three different scenarios (that were discussed in chapter 3 in section 3.5) at the charging station, for the simulation of a PV+ wind system in conjunction with the BESS. The results are compared to see which of the three uses the energy from the HRES to its maximum capacity whilst it uses less energy from the BESS to supply the load demand.

6.3 Resource data and load profile per scenario in Upington

The input data from the two resources, wind and solar, have been collected for one day in a typical day (24 hours) in winter (June) and summer (December) for the proposed energy optimisation model which will be developed. The three load profiles are used as the input to the energy optimisation model developed for each scenario. The load profiles of the Electric Tuk-Tuk vehicle which are given in Table 6.1 below, give a clear indication of the resource availability as well as the load profile per scenario in a 24 hour period.

Table 6.1: Resource data and load profile per scenario

	Summer		**Winter**				
Time(h)	**Solar irradiation** (kWh/m^2/day)	**Wind speed (m/s)**	**Solar irradiation** (kWh/m^2/day)	**Wind speed (m/s)**	**Scenario 1 kW**	**Scenario 2 kW**	**Scenario 3 kW**
00:00	0.000	0.000	0.000	0.459	0.000	0.725	0.725
01:00	0.000	0.000	0.000	0.501	0.000	0.725	0.725
02:00	0.000	0.000	0.000	0.308	0.000	0.725	0.725
03:00	0.000	0.000	0.000	0.233	0.000	0.725	0.725
04:00	0.000	0.000	0.000	0.129	0.000	0.000	0.725
05:00	0.000	0.000	0.000	0.088	0.000	0.000	0.725
06:00	0.000	0.000	0.000	0.062	0.000	0.000	0.725
07:00	0.002	0.000	0.176	0.048	0.000	0.000	0.725
08:00	0.141	0.000	0.251	0.025	0.725	0.000	0.725
09:00	0.417	0.000	0.287	0.011	0.725	0.000	0.725
10:00	0.687	0.000	0.346	0.010	0.725	0.000	0.725
11:00	0.940	0.322	0.438	0.000	0.725	0.000	0.725
12:00	1.062	0.000	0.591	0.000	0.725	0.000	0.725
13:00	1.061	0.000	0.593	0.088	0.725	0.000	0.725
14:00	0.978	0.566	0.492	0.072	0.725	0.000	0.725
15:00	0.846	0.0836	0.351	0.163	0.725	0.000	0.725
16:00	0.679	0.000	0.238	0.256	0.000	0.000	0.725
17:00	0.464	0.000	0.091	0.325	0.000	0.000	0.725
18:00	0.208	0.000	0.000	0.348	0.000	0.000	0.725
19:00	0.043	0.000	0.000	0.366	0.000	0.000	0.725
20:00	0.000	0.0427	0.000	0.416	0.000	0.725	0.725
21:00	0.000	0.222	0.000	0.442	0.000	0.725	0.725
22:00	0.000	0.000	0.000	0.451	0.000	0.725	0.725
23:00	0.000	0.000	0.000	0.468	0.000	0.725	0.725

6.4 System components, sizing and their charging strategies

A mathematical approach for sizing of the main components of the proposed system as well as the charging strategies has already been covered in chapter 3 under sections 3.6 and 3.5 respectively. However, in this chapter only a tabulated summary of the sizes of the hybrid system's components and the different parameters used in the simulations are given, as indicated on Table 6.2 below.

Table 6.2: HRES simulation parameters

Data	**Scenario 1**	**Scenario 2**	**Scenario 3**
Sampling time (Δt)	30 min	30 min	30 min
Load demand per case	5.8 kWh	5.8 kWh	17.4 kWh
Battery maximum SOC	95%	95%	95%
Battery minimum SOC	40%	40%	40%
Battery efficiency kWh/d	85%	85%	85%
PV output energy kWh/d	8.28	0	8.28
Wind output energy kWh/d	0.604	0.236	0.84

6.5 Discussion of simulation results

This section presents the simulated results as well as a discussion. The results that will be discussed are the simulated results of the three scenarios (day charging, night charging and finally all day charging) in one typical day in both summer and winter from a single site in

Upington, to exhibit a scenario that is best suitable in any of the three systems that insures minimal battery usage and maximum usage of the HRES in a charging station. The load profiles in both winter and summer are identical and the only difference is the resources availability.

6.6 Discussion of summer simulation results

In summer the following aspects were observed from the developed model under each scenario.

6.6.1 Scenario 1 load profile results

Figure 6.1 indicates a constant load profile for scenario 1 in summer. In this scenario the Tuk-Tuk is scheduled to initiate its recharging from 08:00 am until 16:00 pm, and in that period the load requirement at the charging station is 0.725 kW per hour for 8 hours which amounts to a total of 5.8 kW power required to meet the load demand.

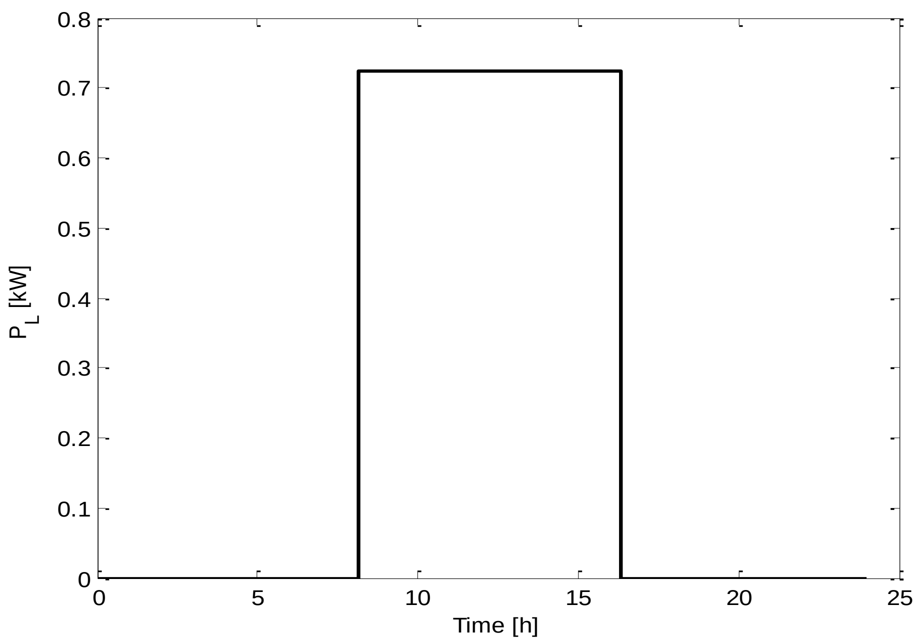

Figure 6.1: Scenario 1 load profile

6.6.1.1 HRES output power flow in summer

HRES output power is the total amount of energy that the resources can produce in a single day; the power output result for these simulation results is taken from Table 6.1. Figures 6.2 and 6.3 represent the HRES's optimal output power flow in 24 hours period in summer. In these two figures it can be noticed that both the P_{PV} and the P_W utilisation are equal to their maximum, and this indicates that the HRES resources are utilised to their maximum capacity.

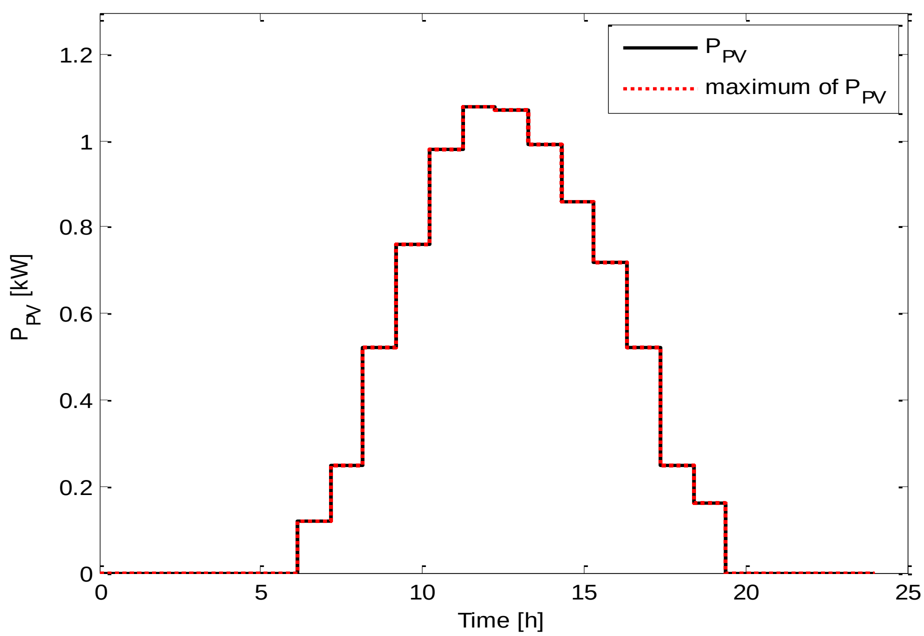

Figure 6.2: PV system resource data in a 24 hour period in summer

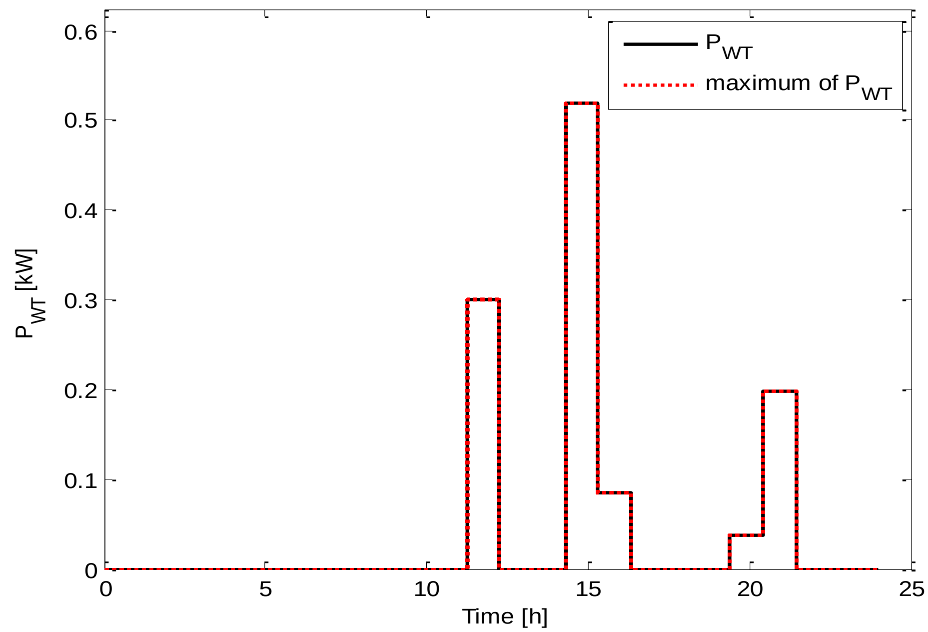

Figure 6.3: Wind system resource data in a 24 hour period in summer

6.6.1.2 Battery power flow for scenario 1 in summer

The battery power flow for scenario 1 in summer is represented by Figure 6.4; the battery is known to be in a charging state when its power falls into the negative region and in a discharging state when its power falls into the positive region. When analysing the battery power flow results representation, it can be observed that only a minimal power output of the battery banks is utilised between 08:00 am and 09:00 am. This is due to the fact that during this time the HRES produces about 77% of the required power for recharging and the other 23% is supplied with the aid of the battery banks (the data for comparisons are taken from Figure 6.2 and Table 6.1 from 08:00 am to 09:00 am, and the data indicate that during that period the resource produced a total of 0.558 kW out of the 0.725 kW required by the load). As the day progresses the load demand is met with the aid of the HRES from 10:00 am until 16:00 pm until all charging activities are concluded at the charging station and the excess electricity is then stored in the battery until there is minimal resource available from the evening, night and early morning before 06:00 am.

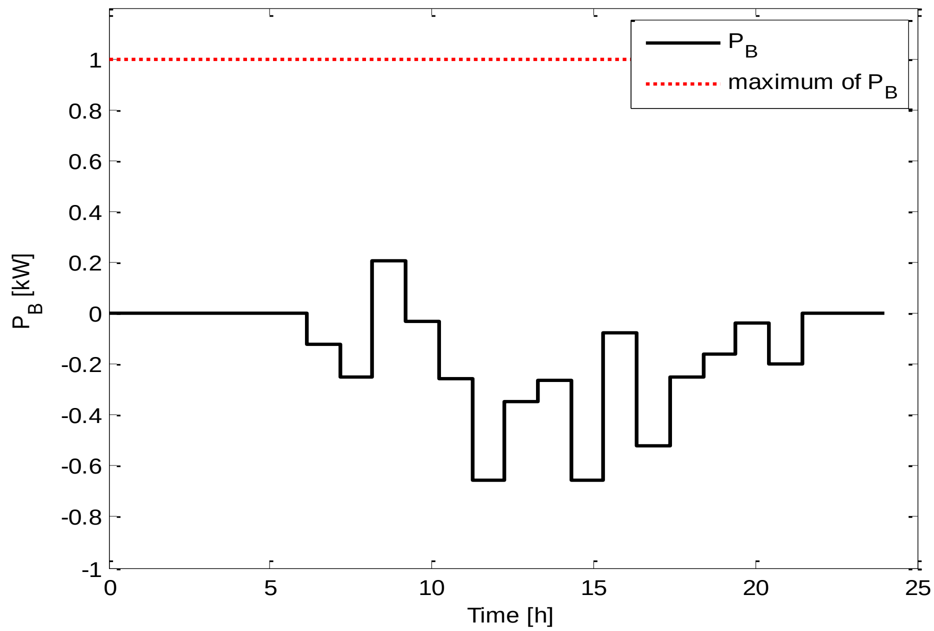

Figure 6.4: The battery power flow for scenario 1in summer

6.6.1.3 Battery state of charge for scenario1 in summer

The simulation result of the battery state of charge for scenario1in summer is represented by Figure 6.5. Before any charging activities resume at the station, the battery is charging from 07:00 am to 08:00 am and as soon as the electric Tuk-Tuk charging is initiated from 08:00 am until 16:00 pm, the battery will only discharge in the morning from 08:00 am to 09:00 am when there is a deficit in the HRES; however, as soon as there is an abundance of energy in the renewable resource then battery is in a charging state. From this simulation it can be observed that the battery operates within the proposed constraints, the battery was observed to be adhering to the proposed constraints whereby it is prohibited to exceed its minimum discharge of 40% and its maximum charge capability of 95%.

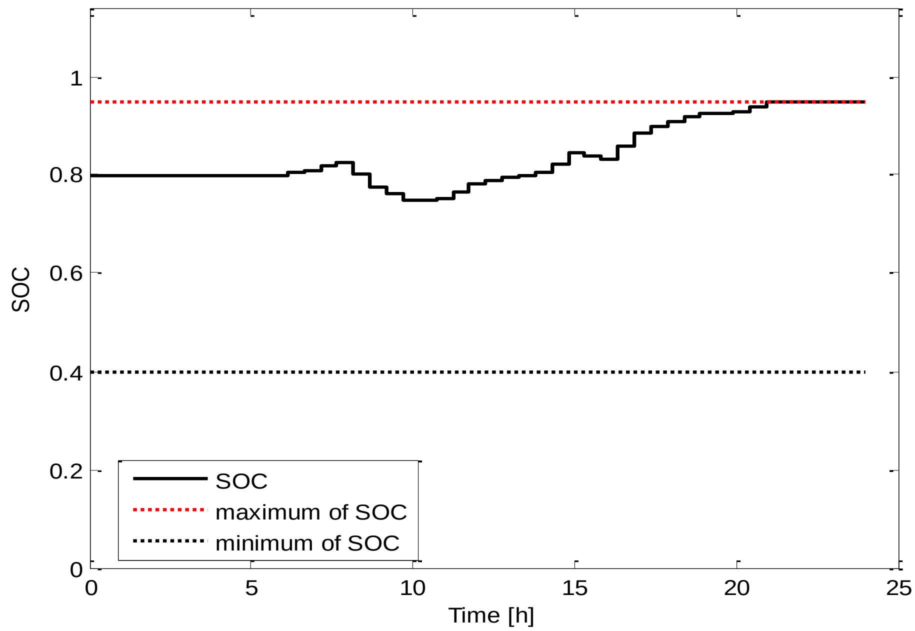

Figure 6.5: The battery state of charge for scenario 1 in summer

6.6.2 Scenario 2 load profile results

Figure 6.6 indicates a constant load profile for scenario 2 in summer. In this scenario the Tuk-Tuk is scheduled to initiate its recharging from 20:00 pm until 04:00 am, and in that duration in that period the load requirement at the charging station is 0.725 kW per hour for 8 hours which amounts to a total of 5.8 kW power required to meet the load demand. The PV and wind systems optimal output power flows are the same as in scenario 1 (refer to Figure 6.2 and 6.3).

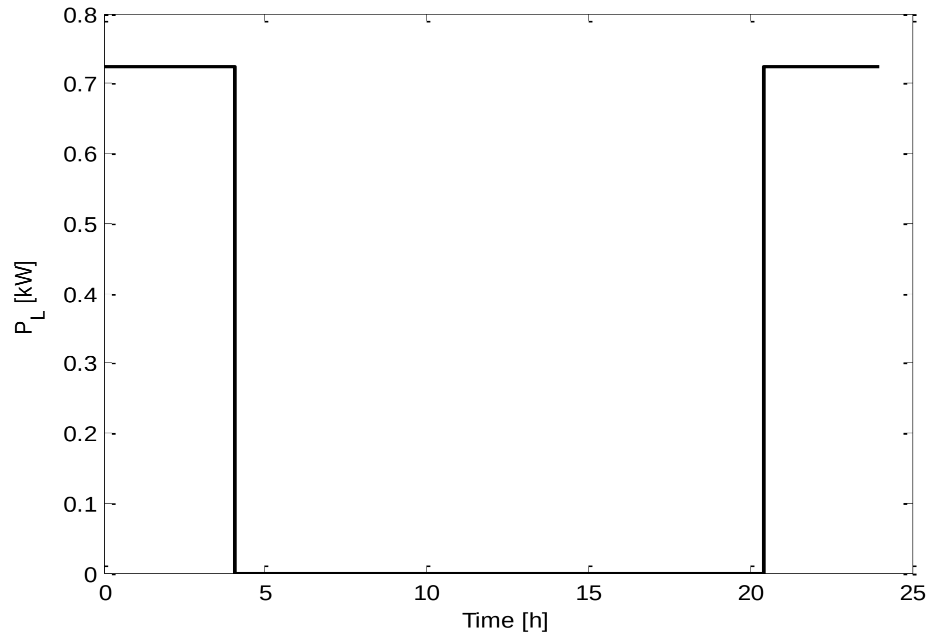

Figure 6.6: Scenario 2 load profile in summer

6.6.2.1 Battery power flow for scenario 2 in summer

The battery power flow for scenario 2 in summer is represented by Figure 6.7. The battery is known to be in a charging state when it falls into the negative region and in a discharging state when it falls in the positive region. The wind system is producing minimal power between 20:00 pm and 22:00 pm. During the night when the sun is absent, the solar system does not generate any power and the load demand is met primarily with aid of a wind system assisted by the battery banks. Between 20:00 pm to 21:00 pm the wind system generates 0.222 kW (31%) of the 0.725 kW required by the load and the remaining 69% in that period is met by the battery bank. From 22:00 pm until 04:00 am the HRES is not generating any power and the load at the charging station is met only by the battery bank, with the power that was stored during the day when there was an abundance of renewable energy resources.

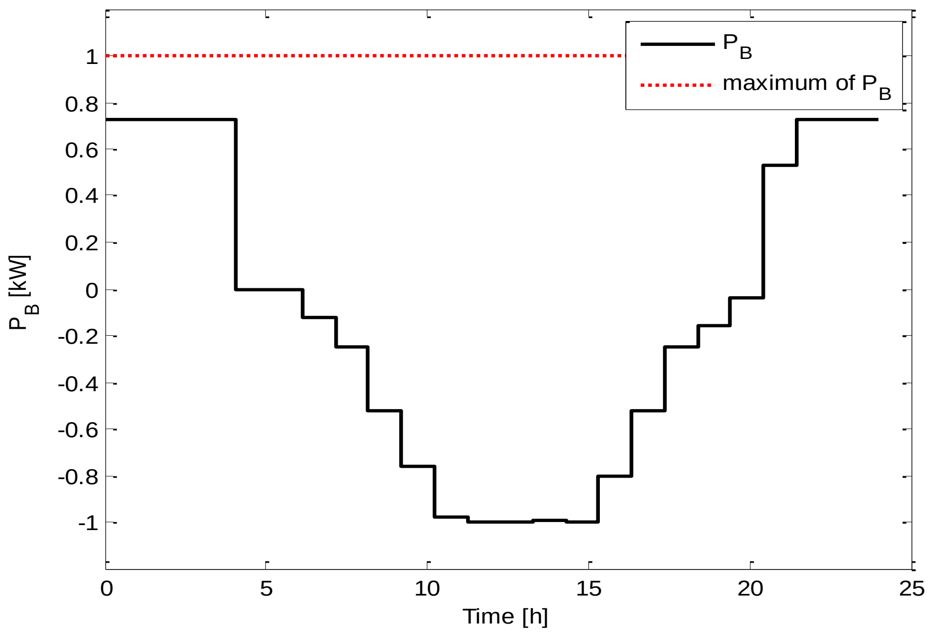

Figure 6.7: The battery power flow for scenario 2 in summer

6.6.2.2 Battery state of charge for scenario 2 in summer

The simulation result for the battery state of charge for scenario 2 in summer is represented in Figure 6.8. Charging at the station starts at 20:00 pm, when the resource potential is at its lowest and during the day when there are no charging activities the generated power is stored in the battery banks. As soon as charging is initiated there is a deficit in the HRES and the battery bank is then utilised to make up for the shortages; in this period the battery is mainly discharged. From this simulation it can be observed that the battery operates within the proposed constraints whereby it is prohibited to exceed its minimum discharge of 40% and its maximum charge capability of 95%.

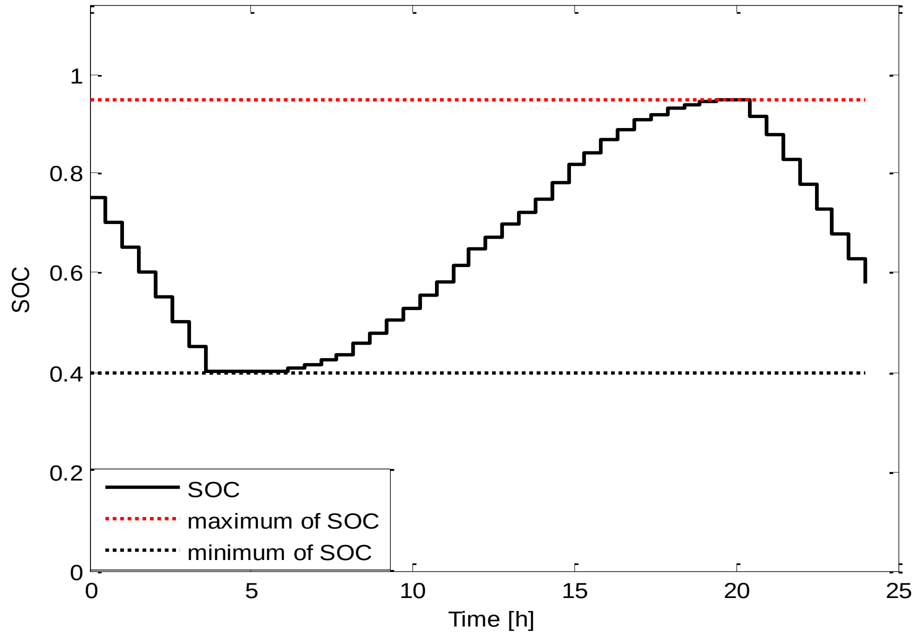

Figure 6.8: The battery state of charge for scenario 2 in summer

6.6.2.3 Scenario 3 load profile results

Figure 6.9 indicates a constant load profile for scenario 3 in summer. In this scenario the Tuk-Tuk is scheduled to initiate its recharging from 00:00 am on day 1 until 00:00 am on day 2 and in that period the load requirement at the charging station is 0.725 kW per hour for 8 hours which amounts to a total of 17.4 kW power required to meet the load demand. The PV and wind system's optimal output power flow are the same as in scenario1 (refer to Figure 6.2 and 6.3).

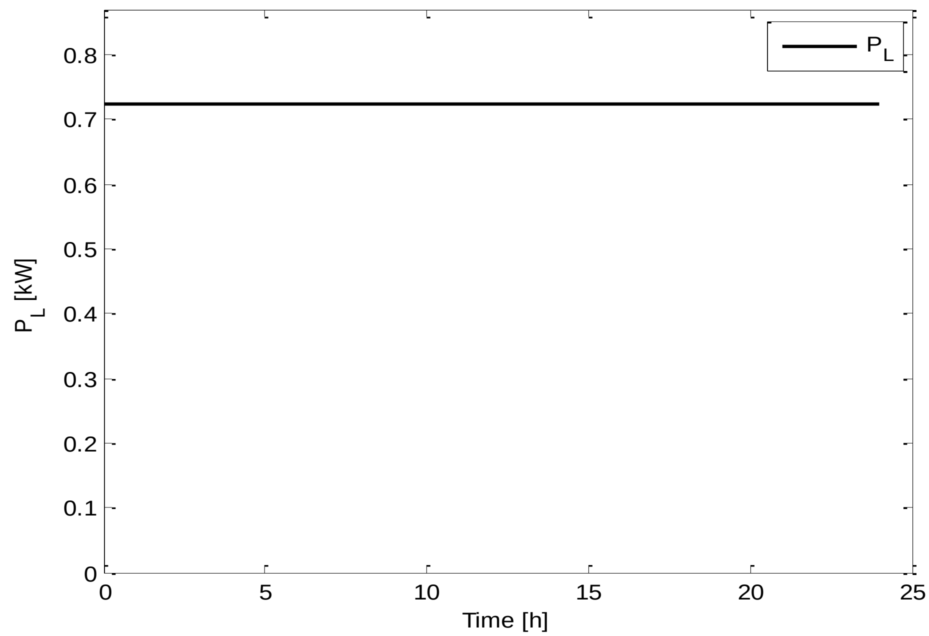

Figure 6.9: Scenario 3 load profile

6.6.2.4 Battery power flow for scenario 3 in summer

The battery power flow for scenario 3 in summer is represented by Figure 6.10. The battery is known to be in a charging state when it falls into the negative region and in a discharging state when it falls into the positive region. When analysing the battery power flow results representation in this figure, it can be observed that both the HRES and battery banks are utilised to their maximum capacity. In this scenario charging takes place from 00:00 am to 00:00 am the next day when each Tuk-Tuk is charged for 8 hours. During the first 8hours from 00:00 am to 08:00 am, when charging is initiated, the load requirement will be primarily catered for by the battery banks as the resources are not generating any power from 00:00 am until 06:00 am, and from 06:00 am to 08:00 am the resource will be responsible for 20% of the load and 80% of the deficit will be met by the battery banks. From 08:00 am to 16:00 pm, when the second Tuk-Tuk is charged, the HRES is assisted by the battery bank for the first three hours, and from 11:00 am until 16:00 pm the HRES is the primary supplier to the Tuk-Tuk. From 16:00 pm to 00:00 am the HRES together with the battery are utilised to adequately meet the load requirements.

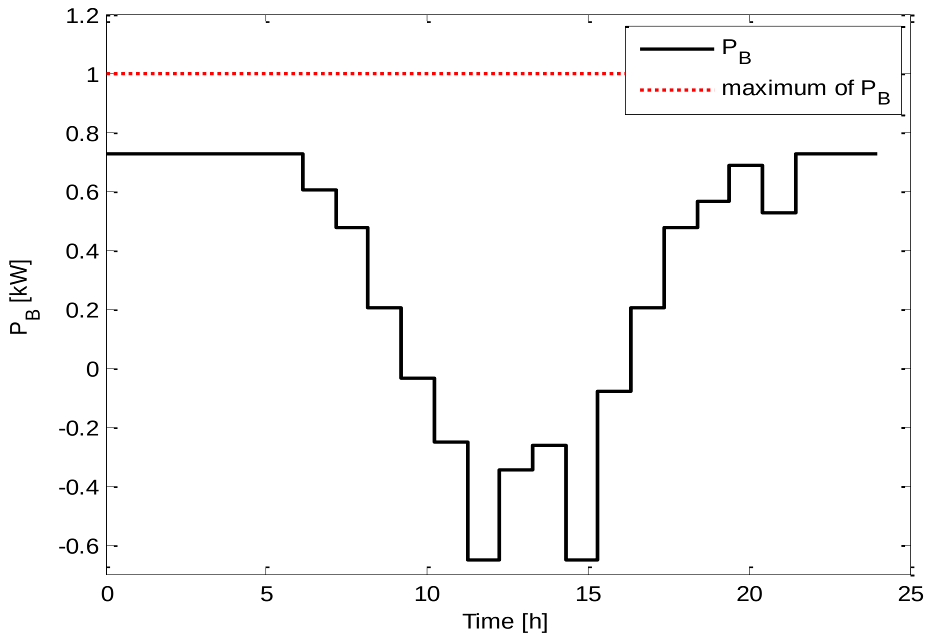

Figure 6.10: The battery power flow for scenario 3 in summer

6.6.2.5 Battery state of charge for scenario 3 in summer

The simulation result for the battery state of charge for scenario 3 in summer is represented by Figure 6.11. From this simulation it can be observed that the battery operates within the proposed constraints, which is 40% minimum discharge and 95% of its maximum charging capacity. The charging station produces 8.765 kW a day and all three Tuk-Tuks requires 17.4 kW a day, meaning that the 50% of the load is met by the HRES and the other 50% will come from the battery. During the 24 hour of non-stop charging of the Tuk-Tuks the battery is charging up when the resources are generating more than the required load, and discharging when there is a deficit in the HRES.

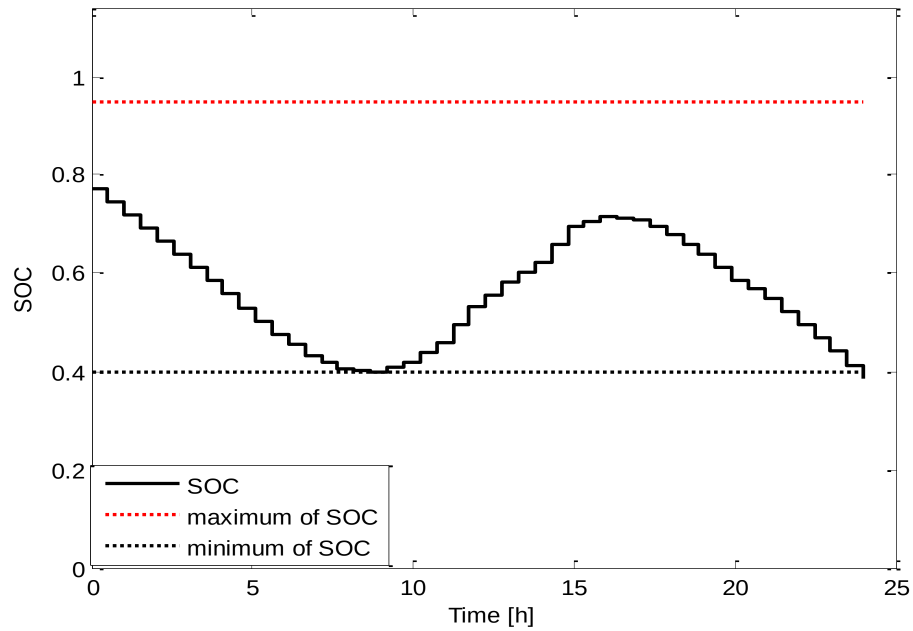

Figure 6.11: The battery state of charge for scenario 3 in summer

6.7 Discussion of winter simulation results

The following results were observed from the developed model under each scenario in winter.

6.7.1 Scenario 1 load profile results

The load profile for scenario 1 is the same as in summer (refer to Figure 6.1), in that the charging activities as well as the charging times are identical.

6.7.1.1 HRES output power flow in winter

Figure 6.12 and 6.13 represents the HRES's optimal output power flow during 24 hours in winter. This is the total amount of energy that the resources can produce in a single day; the power output data for these simulation results are taken from Table 6.1 under winter data. In these two figures it can be noticed that both the P_{PV} and the P_{W} utilisation are equal to their maximum, and this indicates that the HRES resources are utilised to their maximum capacity.

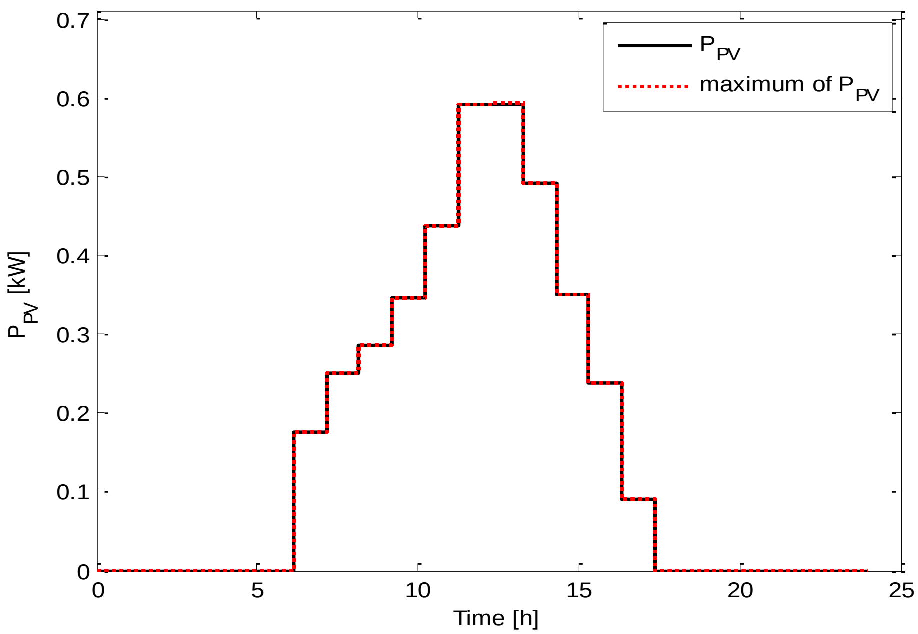

Figure 6.12: PV system resource data in a 24 hour period in winter

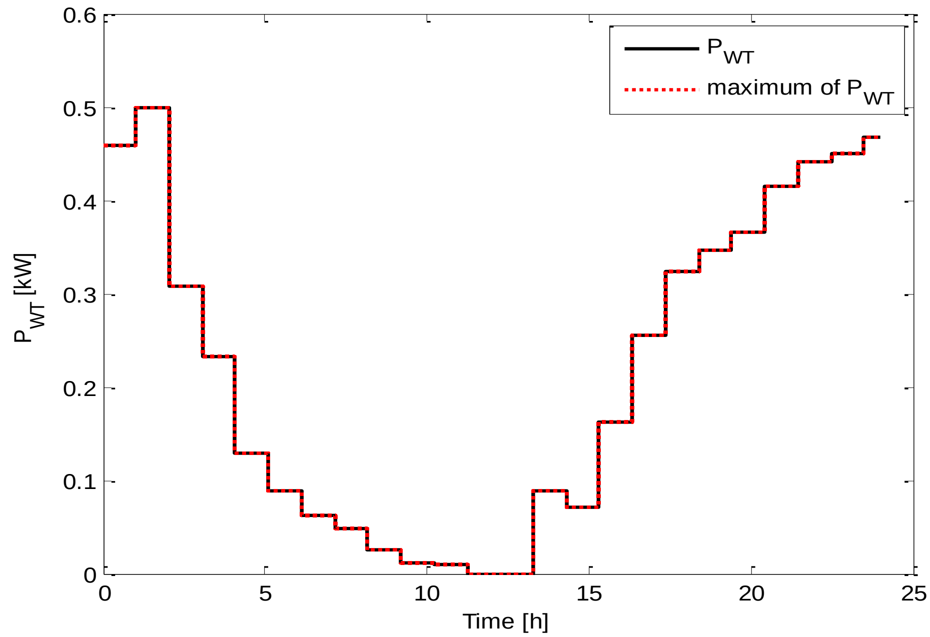

Figure 6.13: Wind system resource data in a 24 hour period in winter

6.7.1.2 Battery power flow for scenario 1 in winter

The battery power flow for scenario 1 in winter is represented by Figure 6.14. The battery is known to be in a charging state when it falls into the negative region and in a discharging state when it falls into the positive region. When analysing the battery power flow results in Figure 6.14, it can be observed that in the early hours of the morning from 00:00 am until 08:00 am the generated power is utilised to charge the battery banks until the electric Tuk-Tuk charging resumes. The charging activities at the charging station begin at 08:00 am when the electric Tuk-Tuk initiates charging, and continue 16:00 pm when the vehicle concludes charging. During the first 4 hours from 08:00 am to 12:00 pm, the HRES is generating 47% (1.368 kW in 4 hours) of the load demand and the remaining 53% (1.532 kW in 4 hours) is supplied from the battery banks, and during the final 4 hours the HRES is now generating 84% (2.436 in 4 hours) of the required energy and the battery banks will supply the minimal deficit of 16% (0.464 kW in 4 hours). Once the electric Tuk-Tuk charging activity ends, the generated energy from the HRES is stored in the battery banks.

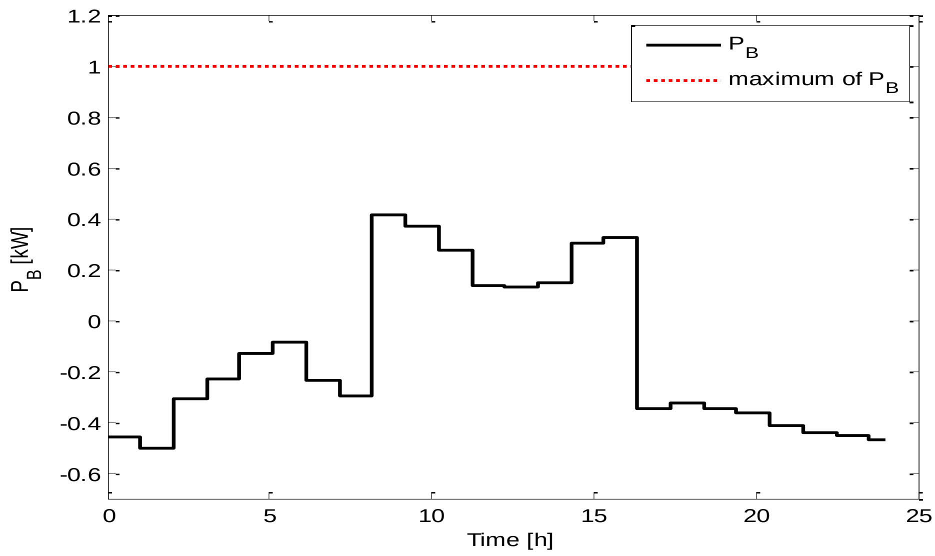

Figure 6.14: The battery power flow for scenario 1 in winter

6.7.1.3 Battery state of charge for scenario1 in winter

The simulation result of the battery state of charge for scenario 1 in winter is represented by Figure 6.15. Before any charging activities resume at the station the battery is charging from 00:00 am to 08:00 am and, as soon as the electric Tuk-Tuk charging is initiated from 08:00 am until 16:00 pm, the battery will be discharging. For the first 4 hours it will be utilised to supply more than the HRES and during the final 4 hours it will be utilised minimally for up to 16% of the required load. From this simulation it can be observed that the battery operates within the proposed constraints, and the battery is observed to be adhering to the proposed constraints in that it is prohibited to exceed its minimum discharge of 40% and its maximum charge capability of 95%.

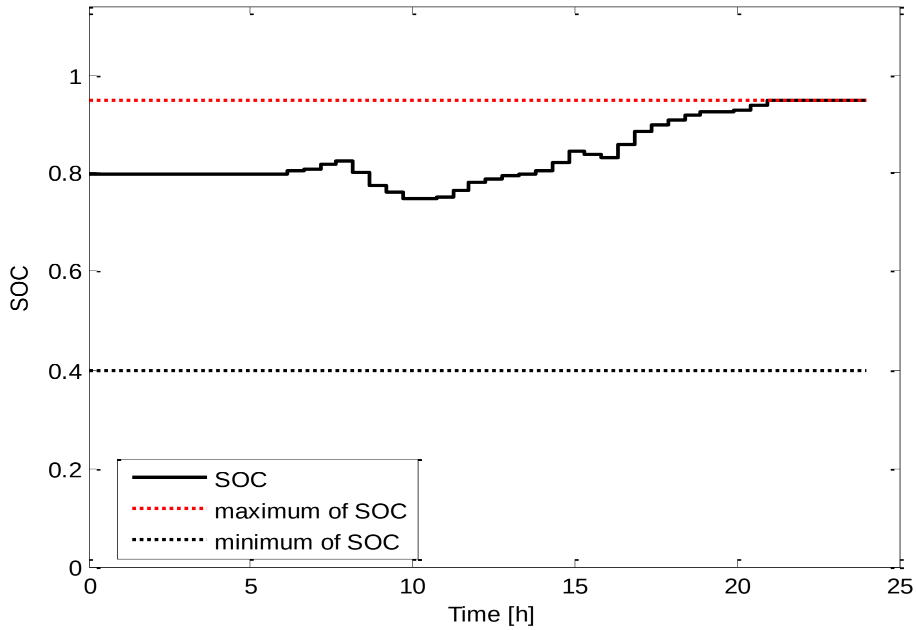

Figure 6.15: The battery state of charge for scenario 1 in winter

6.7.2 Scenario 2 load profile results

The loads profile for scenario 2 is winter is the same as that for scenario 2 in summer (refer to Figure 6.6). The PV and wind systems optimal output power flow are the same as in scenario 1 in winter (refer to Figure 6.12 and 6.13).

6.7.2.1 Battery power flow for scenario 2 in winter

Figure 6.16 illustrated below represents the battery power flow for scenario 2 in winter. The battery is known to be in a charging state when it falls into the negative region and in a discharging state when it falls into the positive region. An observation can be made from analysing figure 6.16 that between 20:00 pm to 04:00 am the load is compensated by the wind power system and battery banks at the charging station, since the PV system is not producing any energy. During the night from 20:00 pm to 00:00 am the wind system is generating 1.777 kW in

4 hours (61% of the load demand 0.725 kW/ h), and the remaining 1.123 kW for 4 hours will be supplied by the battery bank. In the early hours of the morning for the remaining 4 hours of charging the electric Tuk-Tuk, the HRES is generating 52% of the energy and the remaining 48% is supplied by energy from the battery bank. The battery bank is keeping to its proposed constraints of charging up to 95% and discharging down to 40%.

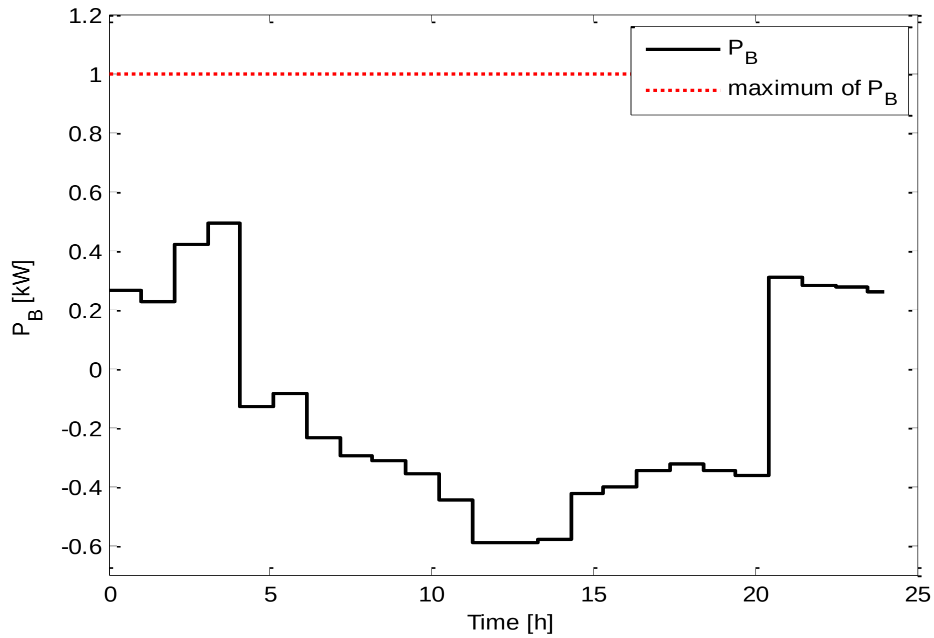

Figure 6.16: The battery power flow for scenario 2 in winter

6.7.2.2 Battery state of charge for scenario 2 in winter

The simulation result for the battery state of charge for scenario 2 in winter is represented by Figure 6.17. From this simulation it can be observed that the battery operates within the proposed constraints, which is 40% minimum discharge and 95% of its maximum charging capacity. Charging at the station starts at 20:00 pm when the resource potential at the charging station is at its highest for the wind system as it generates up to 61% of energy for 4 hours during the night, and as morning approaches from 00:00 am to 04:00 am, the wind system is generating 52% of the load demand energy. During the day when there are no charging activities, the generated power is stored in the battery banks. As soon as charging is initiated there is a deficit in the HRES and the battery bank is then utilised to make up for the shortages; in this period the battery is discharging economically.

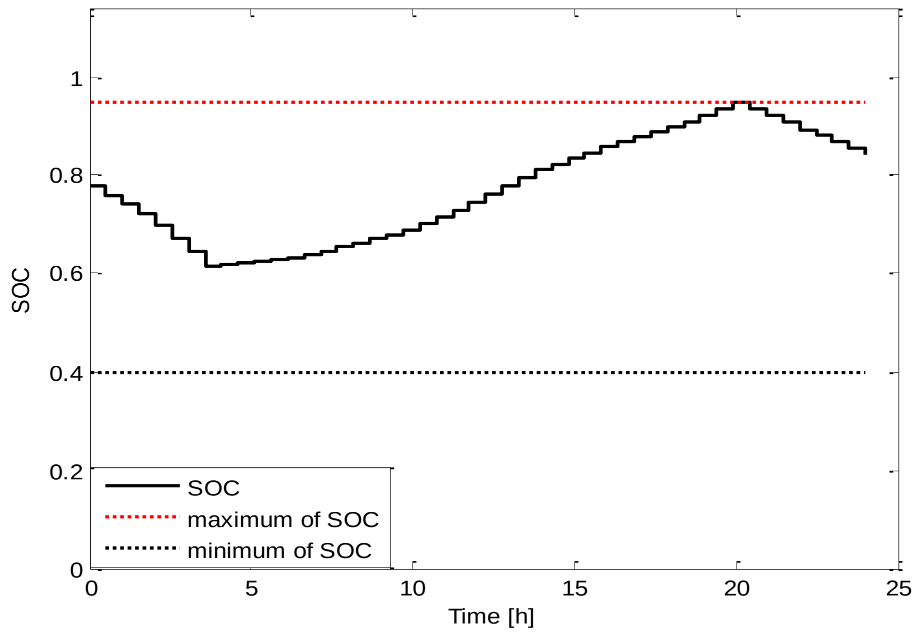

Figure 6.17: The battery state of charge for scenario 2 in winter

6.7.3 Scenario 3 load profile results

The load profile for scenario 3 in winter is the same as that of scenario 3 in summer (refer to Figure 6.9) and the HRES power flow is the same as that of scenarios 1 and 2 in winter (refer to Figures 6.12 and 6.13).

6.7.3.1 Battery power flow for scenario 3 in winter

The battery power flow for scenario 3 in winter is represented by Figure 6.18. The battery is known to be in a charging state when it falls into the negative region and in a discharging state when it falls into the positive region. When analysing the battery power flow results representation in Figure 6.18, it can be observed that both the HRES and battery banks are utilised to their maximum capacity. In this scenario charging takes place from 00:00 am to 00:00 am the next day, when each Tuk-Tuk is charged for 8 hours duration. During the first 8hours from 00:00 am to 08:00 am when charging is initiated, the load requirement will be satisfied by a combination of the wind system and the battery banks as the PV system is not generating any power from 00:00 am until 06:00 am, and from 06:00 am to 08:00 am the resource will be responsible for 39% of the load and 61% of the deficit will be met by the battery banks. From 08:00 am to 16:00 pm when the second Tuk-Tuk is charged, and from 16:00 pm to 00:00 am, the HRES is assisted by the battery bank to supply the Tuk-Tuk with the required energy.

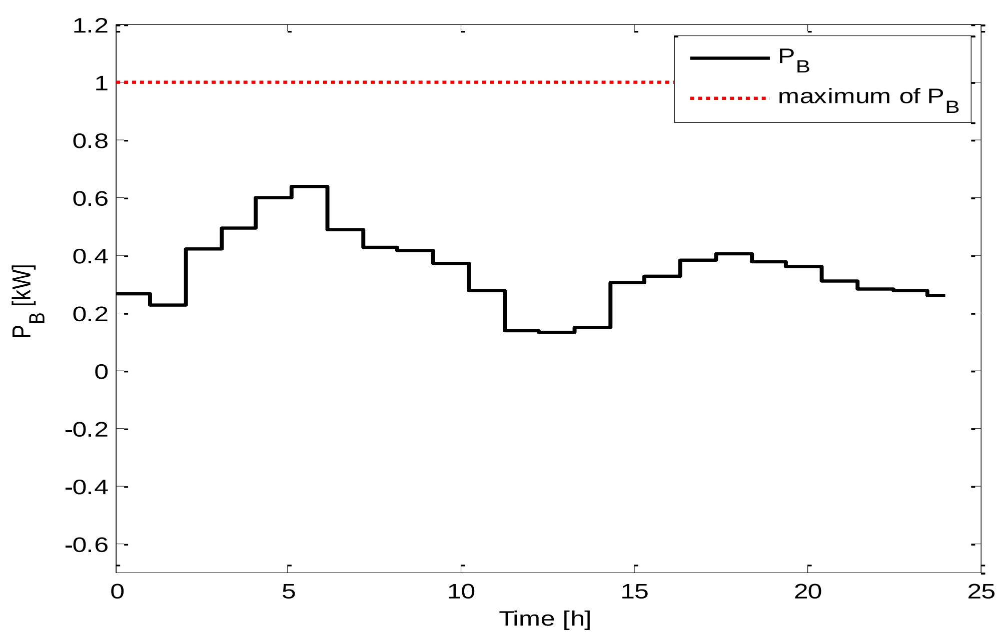

Figure 6.18: The battery power flow for scenario 3 in winter

6.7.3.2 Battery state of charge for scenario 3 in winter

The simulation result for the battery state of charge for scenario 3 in winter is represented by Figure 6.19. From this simulation it can be observed that the battery operates within the proposed constraints, which are 40% minimum discharge and 95% of its maximum charging capacity. The HRES generates 52% of the required power and the remaining 48% then comes from the battery bank as the wind system is the main energy supplier throughout the day when it generates 5.269 kW, a day with the PV only generating 3.854 kW per day. There is frequent discharging of the battery (within its operating limits of 40% and 95%) throughout the day, and this violates the objective function of the proposed model as it requires minimal usage of the battery

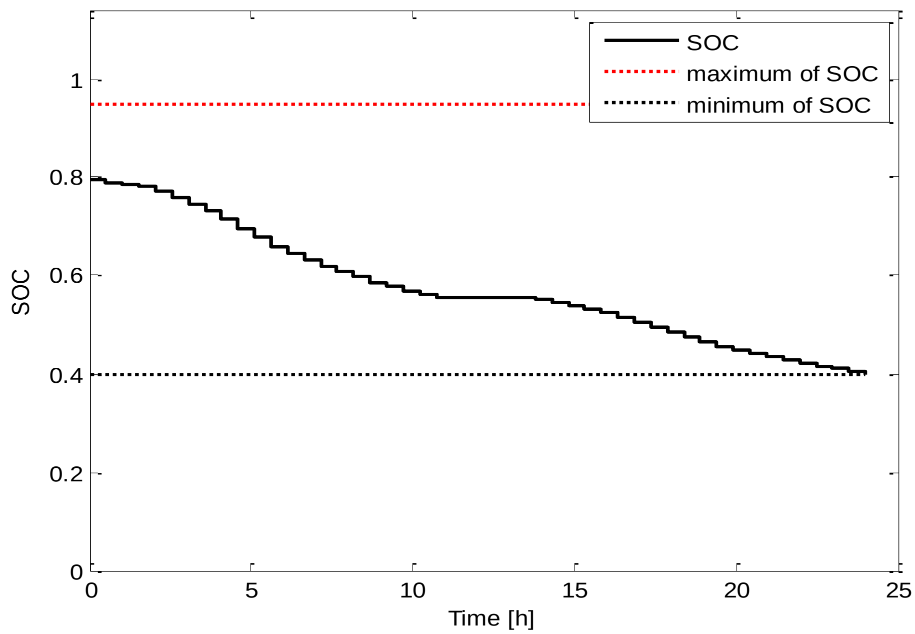

Figure 6.19: The battery state of charge for scenario 3 in winter

6.8 Discussion

The type of load presented in this chapter is a constant load and the battery charging/ discharging capabilities correlates with the constraints that were set in the previous chapter (under section 5.3.3.3). The proposed model (HRES as well as the battery) falls within expected behaviours, validated from similar work by H Tazvinga et al as well as K Kusakana et al [66][67].

6.9 Conclusion

The aim of this chapter was to present the simulation results of the mathematical model for controlling and optimising the daily operation of a standalone hybrid renewable energy charging station. The chapter presented the simulated results in a typical day from both summer and winter regarding the three proposed charging strategies (day charging, night charging and all day charging refer to chapter 3 section 3.5) in Upington. In summer the PV system generates most of the power required to meet the load. The BESS is utilised to meet the load demand when the HRES resources are insufficient to cater for charging at the station. The most viable solution that insures maximum usage of HRES and minimal usage of the battery bank whilst adhering to the proposed constraints is scenario 1 where the load is met primarily by the resources at the charging station. However, before the load increase the battery will experience a minimal discharge to compensate the load in conjunction with HRES.

In winter the generated power at the station is barely enough to maintain the load, so within this season one has to rely on both the HRES and the BESS to avoid any load rejection. Most of the power that is generated at the station is generated from the wind system due to the fact that during the winter season there is a higher wind flow at night than during the day, and the solar irradiation in winter is not as strong as in the summer season. The most suitable solution for this season is given by scenario 1 as 64% of the load is met by HRES and only 36% comes from the battery bank.

Chapter VII: Final conclusion

7.1Final conclusion

This dissertation consisted of two parts: the first part investigated the feasibility of using an electric Tuk-Tuk charging station powered by hybrid renewable energies such as wind and solar in isolated rural parts of South Africa. The second part aimed to develop an optimisation algorithm which ensured maximum usage of the renewable resources and minimal utilisation of the battery bank for supplying the required energy at the electric Tuk-Tuk charging station, without any deficit in the load demand.

As preparation, a background study was conducted with the sole aim of outlining the format for this research must follow. Chapter II, which is a literature review, reviewed previous researcher's inputs regarding electric vehicle technologies, electric vehicle charging station infrastructure, charging standards and the types of connectors available.

Chapter III emphasised the charging station operation strategies and operating principles in a hybrid energy system, which entailed an investigation of the renewable energy potential in the country and surrounding islands so as to evaluate which system configuration and charging strategy would be suitable for each of the three sites that were under investigation, as well as the main components of the HRES and the system configuration, vehicle and load analysis.

Chapter IV investigated the possibilities of using renewable energies for the design of an Electric Tuk-Tuk charging station in the rural areas, and isolated islands of South Africa, with different renewable resource (*solar and wind*), and the results that were simulated then tabulated in three different tables for each respective site. The techno-economic analysis simulations were performed with aid of HOMER and three different strategies were used with one resource configuration (*solar or wind*) respectively, and also a hybrid configuration of both solar and wind. The simulated results illustrate that the type of architecture depends largely on the availability of resources in a certain area/site and also on the most cost-effective scenario that has the lowest cost of energy produced $/kWh for each site.

In chapter V a mathematical model was developed to optimise and control the daily operations of an isolated standalone electric Tuk-Tuk charging station powered by hybrid renewable energies integrated with a battery bank. The model was developed and simulated using fmincon in a MATLAB environment, which ensured a minimal battery usage and maximum HRES utilisation. The optimisation problem was formulated as a multi-objective function with non-linear constraints.

Finally, Chapter VI presented the simulation results which were based on the three scenarios that were discussed in chapter III under section 3.5 simulated in both winter and summer seasons at one location/site (Upington). The simulation results demonstrated that the battery life span can be prolonged by using the developed optimisation model. The difference between the power generated by the HRES and the load demand associated with each respective scenario (scenario 1, 2 and 3), determined the charging and discharging rate of the BESS. The battery control settings (charging and discharging) also played an important role on the operational cost as well as on the battery life itself.

7.2 Suggestions for further research

This dissertation has been presented as part of an on-going research as it does not conclude the work, it is merely a foundation, as other question remains to be answered in relation to the design of a hybrid electric Tuk-Tuk charging station and its optimal control and operational strategies.

This dissertation focused on investigating the possibilities of using an electric Tuk-Tuk battery charging station powered by purely sustainable and renewable energies such as PV and wind incorporated with the BESS and the possibilities of controlling and optimising the daily operation of a standalone hybrid renewable energy in rural areas and research based islands of South Africa.

The simulated model of the electric Tuk-Tuk charging station is mainly focused on two types of resources, which are PV and wind energies. Other models which are powered by other resources, such as hydrokinetic, biomass as well as tidal could also be investigated.

The data for both the proposed system and its control and optimal operational strategies, are acquired differently: The proposed model's data is acquired annually, whereas the optimal and control operation model data are collected on an hourly base. It would be of great interest to simulate both the hybrid system and optimal control in the same day.

The results for both the electric Tuk-Tuk battery charging station and its control and optimisation strategies are simulated. Further studies should be conducted on implementing the real-life time variables for more precise results.

References

[1] How Decent Public Transport Can Strike a Blow to Poverty: Available from http://sacsis.org.za/s/story.php?s=648

, Accessed 23rd July 2013.

[2] B. MERVEN, A. STONE, A. HUGHES AND B COHEN. 2012. Quantifying the energy needs of the transport sector for South Africa: A bottom up model. Working paper 1, pp. 1-28. Available from:

http://www.erc.uct.ac.za/Research/publications/12-Merven-etal_Quantifying_energy_needs_transport%20sector.pdf

, Accessed 23rd July 2013.

[3] S. EJAZ, A. IQBAL, S. RAHMANB, F. BARI, M. ASHRAF, M. NAWAZ, C. LIM AND B. KIM. 2009. Toxicological evaluation of the effects of 2-stroke auto-rickshaw smoke solutions on wound healing. In Environmental Toxicological and Pharmacology. Volume 27 (Issue 3), pp. 373-383.

[4] M. RANA, F. HOSSAIN, S. ROY AND S. KUMAR. 2013. Energy consumption by battery operated rickshaw. In Daffodil International University journal of science and technology. Volume8, Issue2, pp. 72-76.

[5] Nation Master. Environment Statistics of Carbon Dioxide Emissions by Country. Available from:

http://www.nationmaster.com/graph/env_emi-environment-co2-emissions/Kt/Per-capita

, Accessed 10th June 2013.

[6] About SA-Energy: Available from : http://www.info.gov.za/about/energy.htm.

, Accessed 15th June 2013.

[7] List of countries in Africa in co2 per capita. 2014. Available from:
http://www.theguardian.com/news/datablog/2011/jan/31/world-carbon-dioxide-emissions-country-data-co2
, Accessed 15th April 2014.

[8] Understanding the Electric vehicle Landscape to 2020 Available from:
http://www.iea.org/publications/globalevoutlook_2013.pdf.

[9] A. HOLMS AND R. ARGUETA. 2010. A technical report: The electric vehicle. Available from http://www.writing.ucsb.edu/faculty/holms/Writing_2E-_EV_Technical_Research_Report.pdf

[10] 130132_360 Degree Analysis of Electric Vehicles Market_V10_25Jan (2).pdf
, Accessed 18th March 2013.

[11] J. LARMINIE AND J. LOWRY. 2012. Electric vehicle technology explained: 2nd Edition. ISBN: 978-1-119-94273-3. Available from:
http://eu.wiley.com/WileyCDA/WileyTitle/productCd-111994273X.html

[12] H. WANG, Y. FU, R. LI, F. WU AND Q. ZHANG. 2011. Study on key technologies of lithium battery for electric vehicles. In Strategic Technology (IFOST), 6th International Forum, Volume1, pp. 291-294.

[13] K. YUI. 2011. Battery technology of electric vehicle and other green industrial projects. In Power Electronics Systems and Applications (PESA), 4th International Conference, pp. 1-2.

[14] C. CHAN. 2010. An overview of electric vehicle technology. In Proceeding of the IEEE Volume: 81, Issue: 9, pp. 1202-1213.

[15] C. CHANG AND S. WONG. 2004. The state of the art of electric vehicles technology. In Power Electronics and Motion Control Conference, IPEMC 2004. The 4th International conference, Volume 1, pp.46-57.

[16] G. MAGGETO. 2011. A worldwide perspective. In Electric vehicle –A technology Roadmap for the future (Digest No.1998/262), IEEE Colloquium, pp. 1-10.

[17] CEN-CENELEC Focus Group on European Electro-Mobility. 2011. Standardization for road vehicles and associated infrastructure. In Report in response to commission mandate M/468 concerning the charging of electric vehicles, pp. 25- 34, Available from: ftp://ftp.cen.eu/cen/Sectors/List/Transport/Automobile/EV_Report_incl_annexes.pdf **, Accessed 18th June 2013.**

[18] S. LUKIC, P. MULHALL AND E. EMADI. 2008. Energy autonomous solar/battery auto rickshaw. Journal of Asian electric vehicles. Volume 6. Number 2, pp. 1135-1143.

[19] K. KUSAKANA AND H.J VERMAAK. 2014. Design of a photovoltaic-wind charging station for small electric Tuk-Tuk in D.R.Congo. In Renewable Energy for Sustainable Development and Decarbonisation. Volume 67, pp. 40-45.

[20] C. VLAD, M. BANCILA, T. MUNTEANU AND G. MURARIU. 2013. Using renewable energy sources for electric vehicles charging. In *Electrical and Electronics Engineering (ICEEE), 4th International Symposium*, pp. 1-6.

[21] J. INGERSOLL AND G. PERKINS. 1996. The 2.1 kW Photovoltaic Electric vehicle charging station in the city of Santa Monica, California. In Photovoltaic Specialists Conference, Conference Record of the 25th IEEE, pp. 1509 – 1512.

[22] M. ABELLA AND F. CHENLO. 2003. Photovoltaic charging station for electrical vehicles. In 3rd World Conference on Photovoltaic Energy Conversion, Osaka, Japan, pp. 2280-2283.

[23] E. MULJADI, S. DROUILHET, R. HOLZ AND V. VORGIAN. ANALYSIS OF WIND POWER FOR BATTERY CHARGING .Wind Technology Division, National Renewable Energy Laboratory Golden, Colorado.

[24] D. BENZAI AND Z. WANG. 2011. Research on Electric Vehicle Charging Station Technologies Based on a smart Grid. In Power and Energy Engineering Conference (APPEEC), Asia-Pacific, pp. 1-4.

[25] X. WU, Y. DONG, Y. GE AND H. ZHAO. 2013. A high reliable communication technology in Electric vehicle charging station. In Software Security and Reliability-Companion (SERE-C), IEEE International Conference, pp. 198-203.

[26] I. GRAU-UNDA, P. PAPADOPOULOS, S. SKARVELIS-KAZAKOS, L. M. CIPCIGAN AND N. JENKINS (2011). Energy Storage for Balancing a Local Distribution Network Area, Energy Storage in the Emerging Era of Smart Grids, Prof. Rosario Carbone (Ed.), ISBN: 978-953-307-269-2.

[27] S. YANG, J. YAO, T. KANG AND X. ZHU. 2014. Dynamic operation model of the battery swapping station for EV (electric vehicle) in electricity market. In Energy, Volume 65, pp. 544-549.

[28] M. BERTOLUZZO, N. ZABIHI AND G. BUJA. 2012. Overview on battery chargers for plug-in electric vehicles. In Power Electronics and Motion Control Conference (EPE/PEMC), 15th International Conference, pp. Ls4d1-1-Ls4d1-7.

[29] F. LIU, T. NG AND K. CHENG. 2011. A review of international charging coupler standards and its availability in Hong Kong. In Power Electronics Systems and Applications (PESA), 4th International Conference, pp. 1-4.

[30] Y. CHEN, R. YU AND H. DE LA PAMA. 2013. Standardization progress investigation on Electric Vehicle Infrastructure in China. In Hybrid and Electric Vehicle Conference (HEVC2013), IET, pp. 1-6.

[31] M. DELLUCCHI AND T. LIPMAN. 2001. An analysis of the retail and life cost of battery-powered electric vehicles. Transport and Environment Volume no 6. Issue no 6, pp. 371-404 (Elsevier).

[32] M. YILMAZ AND P. KREIN. 2011. Review of battery charger topologies, charging Power levels, and infrastructure for Plug-In Electric and Hybrid vehicles. In Power Electronics, IEEE Transactions (Volume28, Issue 5), pp. 2151-2169.

[33] A. COLLIN, S. DJOKIC, H. THOMAS AND J.MEYER. 2011. Modeling of electric vehicle chargers for power system analysis. In Electronic Power Quality and Utilization (EPQU), 11th International Conference, pp. 1-6.

[34] G. MAURI AND A. VALSECCHI. 2012. A fast charging stations for electric vehicle: The impact on the MV distribution grids of the Milan metropolitan area. In Energy Conference and Exhibition (ENERGCON). IEEE conference publication, pp. 1055-1059.

[35] J. TRABUE, FENGLONG LU AND D.MAKSIMOVIC .2012. Electric vehicle DC charger integrated within a photovoltaic power system. In Applied Power Electronics Conference and Exposition (*APEC), pp. 352 – 358.

[36] A. KUPERMAN, U. LEVY, J. GOVEN, A. ZAFRANSKI AND A. SAVERNINA. 2011. High power Li-Ion battery charger for electric vehicle. In Compatibility and Power Electronics (CPE), 7th International Conference-Workshop pp. 342-347.

[37] R. SHI, X. ZHANG, D. KONG, W. DANG AND P. WONG. 2012. Dynamic impacts of fast-charging stations for electric vehicles on active distribution networks. In Innovative Smart Grid Technologies- Asia (ISGT-Asia), 2012 IEEE conference publication, pp. 1-6.

[38] Wind power and solar power. Available from : http://www.energy.gov.za/files/renewable_frame.html **, Accessed 19th July 2014.**

[39] Solar irradiation in the Middle East. Available from: www.greenrhinoenergy.com/solar/radiation/empiricalevidence.php **, Accessed 29th July 2015.**

[40] J. ASAMOAH .2003. Greening electricity generation in South Africa through wind energy. In greenhouse gas control technologies 6th International Conference, pp. 1349-1352

[41] White paper on the promotion of renewable energy and clean energy development. 2002. Part one-promotion of renewable energy. South Africa: Department of minerals and energy. Available from: http://www.gov.za/sites/www.gov.za/files/rewp220802_2.pdf **, Accessed 20th July 2014.**

[42] Department of Energy South Africa. 2013. Wind resource maps for WASA domain, South Africa. Available from: www.csir.co.za/nationalwindsolarsea/WASA_wind%20resource **, Accessed 20th July 2014.**

[43] K. YOUNG, C. WANG, L. YI WANG, AND K. STRUNZ. 2013. Chapter 2: Electric Vehicle Battery Technologies. *Electric vehicle integration into modern power networks* (Eds.) R. Cracia-Valle and J.A Pecas Lopes, XI, 325. Pp. (s): 15- 43.

[44] T. HOFMAN, S. VAN DER TAS, W. OOMS, E. VAN MEIJL, B. LAUGEMAN. 2009. Development of a micro-hybrid system for a three-wheeled motor taxi. In 24th International battery, hybrid and fuel cell electric vehicle symposium & exposition, Stavanger, Norway.

[45] O. TREMBLAY, L. DESSAINT, A. DEKKICHE. 2007. A generic battery model for the dynamic simulation of hybrid electric vehicles. In Vehicle power and propulsion conference, Montreal, QB.

[46] K. KUSAKANA AND H. VERMAAK. 2011. Hybrid photovoltaic-wind system as power solution for network operators in the D.R.C. In International conference on clean electrical power, pp. 14-16, Ischia, Italy.

[47] A. KAABECHE AND R. IBTIOUEN. 2014. Techno-economic optimization of hybrid photovoltaic/wind/diesel/battery generation in a stand-alone power system. Solar Energy, pp. 171-182.

[48] A. FARD, A. ABUNASRI, A. ZARE AND R. HOSEINZADEH. 2014. Impact of plug-in hybrid electric vehicle charging demands on the optimal energy management of renewable micro-grids. In Energy conference, Volume 78, pp. 904-915.

[49] A. PACHORI AND P. SUHANE. 2014. Design and modeling of standalone hybrid power system with MATLAB/simulink. In International Journal of Scientific Research and Management Studies (IJSRMS) Volume 1 (Issue) *2*, pp. 65-71.

[50] S. DIAF, D. DIAF, M. BELHAMEL, M. HADDADI AND A. LOUCHE. 2007. A methodology for optimal sizing of autonomous hybrid PV/Wind system. Energy Policy 35, pp5708-5718.

[51] A. BELFKIRA, L. ZHANG AND G. BARAKAT. 2011. Optimal sizing study of hybrid/ Wind/PV/Diesel power generation unit. Solar Energy 85, pp. 100-110.

[52] O. ERDINC AND M. UZUNOGLU. 2012. Optimum design of hybrid renewable energy systems: Overview of different Approaches. In Renewable and Sustainable Energy Reviews, Volume 16, (Issue 3), pp. 1412– 1425.

[53] A. MALEKI AND A. ASKARZADEH. 2014. Optimal sizing of a PV/wind/diesel system with battery storage for electrification to an off-grid remote region: A case study of Rafsanjani, Iran. In Sustainable Energy Technologies and Assessments, no7, pp. 147–153.

[54] J. LI, W. WEI AND J. XIANG. 2012. A Simple Sizing Algorithm for Stand-Alone PV/Wind/Battery Hybrid Micro grids. In Energies, *Volume 5*, pp. 5307-5323.

[55] B. XIAO, Y. SHI AND L. HE. 2010. A universal state-of-charge algorithm for batteries. In the 47th ACM/IEEE Design Automation Conference, (DAC), pp. 687-692.

[56] M. BEHZADI AND M. NIASATI. 2015. Comparative performance analysis of a hybrid PV/FC/battery stand-alone system using different power management strategies and sizing approaches. International journal of hydrogen energy, Volume 40 (Issue 1), pp. 538-548.

[57] A. GUDELJ AND M. KRČUM. 2013. Simulation and Optimization of Independent Renewable Energy Hybrid System. In Transactions on maritime science Trans. Available from: http://hrcak.srce.hr/file/148130.

[58] X. ZHANG, S. TAN, G. LI, J. LI AND Z. FENG. 2013. Components sizing of hybrid energy systems via the optimization of power dispatch simulations. In Energy 52, pp. 165-172.

[59] H. TAZVINGA, B. ZHU, X. XIA. 2014. Energy dispatch strategies for a photovoltaic-wind-diesel-battery hybrid power system. In Solar Energy. 108, pp. 412-420.

[60] J. LESAGE AND R. LONGORIA. 2013. Hybrid observer design for online battery state of charge estimation" IEEE, In American Control Conference, pp. 1994-1999.

[61] Global optimization tool box. Available from: www.mathworks.com/datasheets/pdf/global-optimization-toolbox.pdf **, Accessed 18th May 2015.**

[62] D. MEJIA. 2011. Optimization of a stand-alone hybrid wind/solar generation system for lifespan extension. A thesis submitted to the University of Colorado Denver in partial fulfillment of the requirements for the degree of Masters of Science Electrical Engineering Electrical Engineering 2011.

[63] Dynamic programming. Available from : http://web.mit.edu/15.053/www/AMP-Chapter-11.pdf **, Accessed 18th May 2015.**

[64] Quasi-Newton methods. Available form: http://terminus.sdsu.edu/SDSU/Math693a_f2013/Lectures/18/lecture.pdf **, Accessed 18th May 2015.**

[65] I. ZADEH. 1965. Fuzzy sets. Information and control. Volume 8, Issue3, pp. 338-353 Available from: http://dx.doi.org/10.1016/S0019-9958(65)90241-X **, Accessed 18th May 2015.**

[66] H. TAZVINGA, X XIA, J ZHANG. 2013. Minimum cost solution of photovoltaic–diesel–battery hybrid power systems for remote consumers. Solar energy 96, pp. 292-299.

[67] K. KUSAKANA. 2015. Optimal scheduled power flow for distributed photovoltaic/wind/diesel generators with battery storage system. IET Renewable Power Generation. DOI: 10.1049/iet-rpg.2015.0027.

Appendices

Appendix A: Selected optimal operation control program (using fmincon)

```
Delta T=30;

%sampling time in minutes

hours=24;

N=hours*60/deltaT;

soc_max=0.95;

soc_min= 0.4;

soc_0=0.8;

Eff=0.8;

En=19800;

K=(deltaT*Eff)/En; %data needed

PPV_max=[0*ones(1,N/24),0*ones(1,N/24),0*ones(1,N/24),0*ones(1,N/24),0*ones(1,N/24),0*ones(1,N/24),0.176*ones(1,N/24),0.251*ones(1,N/24),0.287*ones(1,N/24),0.346*ones(1,N/24),0.438*ones(1,N/24),0.591*ones(1,N/24),0.593*ones(1,N/24),0.492*ones(1,N/24),0.351*ones(1,N/24),0.238*ones(1,N/24),0.091*ones(1,N/24),0*ones(1,N/24),0*ones(1,N/24),0*ones(1,N/24),0*ones(1,N/24),0*ones(1,N/24),0*ones(1,N/24),0*ones(1,N/24)]';

PWT_max=[0.459*ones(1,N/24), 0.501*ones(1,N/24), 0.308*ones(1,N/24), 0.233*ones(1,N/24), 0.129*ones(1,N/24), 0.088*ones(1,N/24), 0.062*ones(1,N/24), 0.048*ones(1,N/24), 0.025*ones(1,N/24), 0.011*ones(1,N/24), 0.010*ones(1,N/24), 0*ones(1,N/24), 0*ones(1,N/24), 0.088*ones(1,N/24), 0.072*ones(1,N/24), 0.163*ones(1,N/24), 0.256*ones(1,N/24),
```

```
0.325*ones(1,N/24), 0.348*ones(1,N/24), 0.366*ones(1,N/24), 0.416*ones(1,N/24),
0.442*ones(1,N/24), 0.451*ones(1,N/24), 0.468*ones(1,N/24)]';
PL_max=[0*ones(1,N/24),0*ones(1,N/24),0*ones(1,N/24),0*ones(1,N/24),0*ones(1,N/24),0*on
es(1,N/24),0*ones(1,N/24),0*ones(1,N/24),0.725*ones(1,N/24),0.725*ones(1,N/24),0.725*ones(
1,N/24),0.725*ones(1,N/24),0.725*ones(1,N/24),0.725*ones(1,N/24),0.725*ones(1,N/24),0.725
*ones(1,N/24),0*ones(1,N/24),0*ones(1,N/24),0*ones(1,N/24),0*ones(1,N/24),0*ones(1,N/24),0
*ones(1,N/24),0*ones(1,N/24),0*ones(1,N/24)];
PB_max=1;
%test = ones(N,N);
A1=[zeros(N,N),zeros(N,N),-K*tril(ones(N,N))];
A2=[zeros(N,N),zeros(N,N),K*tril(ones(N,N))];
A=[A1;A2];
b1=(soc_max- soc_0)*ones(N,1);
b2=(soc_0-soc_min)*ones(N,1);
b=[b1,b2];
Aeq=[eye(N,N),eye(N,N),eye(N,N)];
beq= PL_max(1:N);
lb=[zeros(N,1),zeros(N,1),-PB_max*ones(N,1)];
ub=[PPV_max(1:N),PWT_max(1:N),PB_max*ones(N,1)];
x0=ub;

options=optimset('Algorithm','interior-point');
 optnew=optimset(options,'MaxFunEvals',90000,'Tolx',1e-8);
```

```
x = fmincon(@obj_lindi1,x0,A,b,Aeq,beq,lb,ub,[],optnew);

%exctract different variable vectors
P_PV=x(1:N);
P_WT=x(N+1:2*N);
P_B=x(2*N+1:3*N);

%state of battery extraction
for i=1:N
 soc(i)=soc_0-K*P_B(i);
 soc_0=soc(i);
end
soc1=soc(1:N);
%plots

%load profile
figure (1)
stairs(linspace(0,hours,N),PL_max(1:N),'k','linewidth',1.5)
ylabel('P_L [kW]')
xlabel('Time [h]')
% PV
figure (2)
```

```
stairs(linspace(0,hours,N),P_PV(1:N),'k','linewidth',1.5)

hold on

stairs(linspace(0,hours,N),PPV_max*ones(1,N),':r','linewidth',1.5)

ylabel('P_P_V [kW]')

xlabel('Time [h]')

legend('P_P_V','maximum of P_P_V')

axis([0 hours+1 0 1.2*max(PPV_max)]);

% Wind

figure (3)

stairs(linspace(0,hours,N),P_WT(1:N),'k','linewidth',1.5)

hold on

stairs(linspace(0,hours,N),PWT_max*ones(1,N),':r','linewidth',1.5)

ylabel('P_W_T [kW]')

xlabel('Time [h]')

legend('P_W_T','maximum of P_W_T')

axis([0 hours+1 0 1.2*max(PWT_max)]);


% Battery bank

figure (4)

stairs(linspace(0,hours,N),P_B(1:N),'k','linewidth',1.5)

hold on

stairs(linspace(0,hours,N),PB_max*ones(1,N),':r','linewidth',1.5)

ylabel('P_B [kW]')
```

```
xlabel('Time [h]')
legend('P_B','maximum of P_B')
axis([0 hours+1 -0.7 1.2*max(PB_max)]);

%SOC
Figure (5)
stairs (linspace(0,hours,N),soc1(1:N),'k','linewidth',1.5)
hold on
stairs(linspace(0,hours,N),soc_max*ones(1,N),':r','linewidth',1.5)
hold on
stairs(linspace(0,hours,N),soc_min*ones(1,N),':k','linewidth',1.5)
ylabel('SOC')
axis([0 hours+1 0 1.2*max(soc_max)]);
xlabel('Time [h]')
legend('SOC','maximum of SOC','minimum of SOC')
```